

**SUM-RATE OPTIMAL RESOURCE ALLOCATION FOR
SINGLE CARRIER FREQUENCY DIVISION MULTIPLE ACCESS SYSTEMS**

M.Sc. THESIS

Teoman MERT

Department of Electronics & Communication Engineering

Telecommunication Engineering Programme

JUNE 2013

**SUM-RATE OPTIMAL RESOURCE ALLOCATION FOR
SINGLE CARRIER FREQUENCY DIVISION MULTIPLE ACCESS SYSTEMS**

M.Sc. THESIS

**Teoman MERT
(504101327)**

Department of Electronics & Communication Engineering

Telecommunication Engineering Programme

Thesis Advisor: Prof. Dr. Hakan Ali ÇIRPAN

JUNE 2013

**TEK TAŞIYICILI FREKANS BÖLMELİ ÇOKLU ERİŞİM
SİSTEMLERİ İÇİN TOPLAM VERİ HIZINI
ENBÜYÜKLEYEN ÖZKAYNAK TAHSİSİ**

YÜKSEK LİSANS TEZİ

**Teoman MERT
(504101327)**

Elektronik ve Haberleşme Mühendisliği Anabilim Dalı

Telekomünikasyon Mühendisliği Programı

Tez Danışmanı: Prof. Dr. Hakan Ali ÇIRPAN

HAZİRAN 2013

Teoman MERT, a **M.Sc.** student of **ITU Institute of Science and Technology** student ID **504101327**, successfully defended the **thesis** entitled “**SUM-RATE OPTIMAL RESOURCE ALLOCATION FOR SINGLE CARRIER FREQUENCY DIVISION MULTIPLE ACCESS SYSTEMS**”, which he prepared after fulfilling the requirements specified in the associated legislations, before the jury whose signatures are below.

Thesis Advisor : **Prof. Dr. Hakan Ali ÇIRPAN**
Istanbul Technical University

Jury Members : **Assoc. Prof. Dr. Onur KAYA**
Işık University

Assoc. Prof. Dr. Güneş KARABULUT KURT
Istanbul Technical University

Date of Submission : **3 May 2013**

Date of Defense : **6 June 2013**

To my family,

FOREWORD

First of all, I would like to express my deepest acknowledgements to my supervisor Prof. Dr. Hakan Ali ÇIRPAN for his support and guidance throughout my thesis work. Besides, I would like to express my appreciation to Assoc. Prof. Dr. Onur KAYA for his invaluable guidance and encouragement throughout my research study. I would like to my friends and colleagues for their support and constructive suggestions on this thesis.

I would also like to express my profound gratitude to my family for their endless love, encouragement and motivation.

Finally, I would like to thank TÜBİTAK (The Scientific and Technological Research Council of Turkey) for providing me scholarship during my M.Sc. study.

June 2013

Teoman MERT
Electrical and Electronics Engineer

TABLE OF CONTENTS

| | <u>Page</u> |
|---|-------------|
| FOREWORD | ix |
| TABLE OF CONTENTS | xi |
| ABBREVIATIONS | xiii |
| LIST OF TABLES | xv |
| LIST OF FIGURES | xvii |
| SUMMARY | xix |
| ÖZET | xxi |
| 1. INTRODUCTION | 1 |
| 1.1 Literature Review | 2 |
| 1.2 Purpose of the Thesis..... | 4 |
| 1.3 Preview of the Thesis..... | 4 |
| 2. BACKGROUND THEORY | 5 |
| 2.1 Channel Characteristics | 5 |
| 2.1.1 Transmit and receive signal models..... | 5 |
| 2.1.2 Large scale propagation model..... | 6 |
| 2.1.2.1 Path loss | 6 |
| 2.1.2.2 Shadowing | 7 |
| 2.1.3 Small scale propagation model..... | 8 |
| 2.1.3.1 Coherence time and bandwidth | 9 |
| 2.1.3.2 Types of small scale fading..... | 10 |
| Small scale fading: slow fading vs. fast fading..... | 10 |
| Small scale fading: frequency-selective fading vs. flat fading..... | 11 |
| 2.2 Capacity and Gaussian Channel | 12 |
| 2.2.1 Capacity of a bandlimited channel | 15 |
| 2.2.2 Parallel Gaussian channel..... | 16 |
| 2.3 Optimization Problems | 18 |
| 2.3.1 Convex optimization problems | 18 |
| 2.3.2 Concave maximization problems | 19 |
| 2.3.3 Karush-Kuhn-Tucker optimality conditions | 19 |
| 3. FREQUENCY MULTIPLEXING AND SINGLE CARRIER FDMA | 21 |
| 3.1 Frequency Multiplexing | 21 |
| 3.1.1 Orthogonal frequency division multiplexing..... | 21 |
| 3.1.1.1 OFDM: signal processing | 22 |
| 3.1.2 Single carrier modulation with frequency domain equalization..... | 24 |
| 3.1.3 Comparison of OFDM and SC/FDE | 27 |

| | |
|---|-----------|
| 3.2 Single Carrier FDMA | 27 |
| 3.2.1 SC-FDMA: block diagram | 29 |
| 3.2.2 SC-FDMA: signal processing..... | 32 |
| 3.2.3 Comparison with OFDMA | 34 |
| 3.2.4 Subcarrier mapping | 36 |
| 3.2.5 Peak-to-average-power ratio of SC-FDMA..... | 37 |
| 4. SUM-RATE OPTIMAL RESOURCE ALLOCATION | 41 |
| 4.1 Introduction | 41 |
| 4.2 System Model..... | 42 |
| 4.3 Joint Power and Chunk Allocation..... | 44 |
| 4.3.1 Optimal power allocation | 46 |
| 4.3.2 Optimal and suboptimal chunk allocation..... | 49 |
| 5. SIMULATIONS AND RESULTS..... | 53 |
| 5.1 Sum-Rate Capacity Simulations..... | 53 |
| 5.2 PAPR Analysis of Proposed Power Allocation Algorithm..... | 59 |
| 6. CONCLUSIONS AND FUTURE WORKS..... | 61 |
| REFERENCES..... | 63 |
| APPENDICES | 67 |
| 8. APPENDIX A.1..... | 69 |
| CURRICULUM VITAE..... | 71 |

ABBREVIATIONS

| | |
|----------------|---|
| 3GPP | : 3rd Generation Partnership Project |
| ADC | : Analog-to-Digital Converter |
| AWGN | : Additive White Gaussian Noise |
| BPSK | : Binary Phase-Shift Keying |
| CP | : Cyclic Prefix |
| CSI | : Channel State Information |
| DFT | : Discrete Fourier Transform |
| FDMA | : Frequency Division Multiple Access |
| FFT | : Fast Fourier Transform |
| IBI | : Inter-Block Interference |
| IDFT | : Inverse Discrete Fourier Transform |
| IFDMA | : Interleaved Frequency Division Multiple Access |
| IFFT | : Inverse Fast Fourier Transform |
| IID | : Independent and Identically Distributed |
| ISI | : Inter-symbol Interference |
| KKT | : Karush Kuhn Tucker |
| LFDMA | : Localized Frequency Division Multiple Access |
| LOS | : Line of Sight |
| LTE | : Long-Term Evolution |
| OFDM | : Orthogonal Frequency-Division Multiplexing |
| OFDMA | : Orthogonal Frequency-Division Multiple Access |
| QAM | : Quadrature Amplitude Modulation |
| QPSK | : Quadrature Phase Shift Keying |
| PAPR | : Peak-to-Average Power Ratio |
| R-IFDMA | : Round Robin IFDMA |
| R-LFDMA | : Round Robin LFDMA |
| RF | : Radio Frequency |
| SC/FDE | : Single Carrier/Frequency Domain Equalization |
| SC-FDMA | : Single Carrier Frequency Division Multiple Access |
| SNR | : Signal-to-Noise Ratio |
| V-MIMO | : Virtual Multiple Input Multiple Output |
| WiMAX | : Worldwide Interoperability for Microwave Access |

LIST OF TABLES

| | <u>Page</u> |
|---|-------------|
| Table 3.1 : Comparison between OFDM and SC/FDE | 28 |

LIST OF FIGURES

| | <u>Page</u> |
|--|-------------|
| Figure 2.1 : Multipath, shadowing and path loss versus distance | 6 |
| Figure 2.2 : Types of small scale fading..... | 10 |
| Figure 2.3 : Gaussian channel | 13 |
| Figure 2.4 : Waterfilling technique for parallel channels | 17 |
| Figure 3.1 : A general multi-carrier modulation system..... | 22 |
| Figure 3.2 : Essential OFDM signal processing..... | 22 |
| Figure 3.3 : Cyclic prefix | 24 |
| Figure 3.4 : Basic idea behind FDE | 25 |
| Figure 3.5 : Block diagrams of SC/FDE and OFDM systems | 26 |
| Figure 3.6 : OFDM and SC/FDE receivers | 27 |
| Figure 3.7 : Transmitter and receiver structure of SC-FDMA and OFDMA systems..... | 31 |
| Figure 3.8 : Generation of SC-FDMA transmit symbol | 32 |
| Figure 3.9 : Raised-cosine filter | 34 |
| Figure 3.10 : SC-FDMA receiver structure from a multiple user access perspective with Q terminals in the uplink | 35 |
| Figure 3.11 : Comparison of SC-FDMA and OFDMA transmit sequence of QPSK symbols..... | 36 |
| Figure 3.12 : Types of SC-FDMA subcarrier mapping..... | 37 |
| Figure 3.13 : An example of SC-FDMA symbol in frequency domain..... | 38 |
| Figure 3.14 : An example of SC-FDMA transmit symbols in the time domain | 38 |
| Figure 4.1 : Channel impulse response of two different user..... | 42 |
| Figure 4.2 : Bipartite graph representing matching of users and chunks..... | 50 |
| Figure 5.1 : Sum rate of proposed algorithms (SNR=-5dB, $N=16$ chunks, $B=5$ MHz, $L=256$ subcarriers, 8-tap Rayleigh channel) | 55 |
| Figure 5.2 : Sum rate of proposed algorithms (SNR=-5dB, $N=16$ chunks, $B=5$ MHz, $L=256$, subcarriers, 10-tap Rayleigh channel) | 56 |
| Figure 5.3 : Sum rate of proposed algorithms (SNR=-5dB, $N=16$ chunks, $B=5$ MHz, $L=256$, subcarriers, 20-tap Rayleigh channel) | 56 |
| Figure 5.4 : Sum rate of proposed algorithms (SNR=-5dB, $N=16$ chunks, $B=5$ MHz, $L=256$, subcarriers, 40-tap Rayleigh channel) | 56 |
| Figure 5.5 : Sum rate of proposed algorithms (SNR=-5dB, $N=16$ chunks, $B=5$ MHz, $L=256$, subcarriers, 60-tap Rayleigh channel) | 57 |
| Figure 5.6 : Sum rate of proposed algorithms (SNR=-5dB, $N=32$ chunks, $B=10$ MHz, $L=512$, subcarriers, 8-tap Rayleigh channel) | 57 |

Figure 5.7 : Sum rate of proposed algorithms (SNR=-5dB, $N=32$ chunks, $B=10\text{MHz}$, $L=512$, subcarriers, 10-tap Rayleigh channel) 57

Figure 5.8 : Sum rate of proposed algorithms (SNR=-5dB, $N=32$ chunks, $B=10\text{MHz}$, $L=512$, subcarriers, 20-tap Rayleigh channel) 58

Figure 5.9 : Sum rate of proposed algorithms (SNR=-5dB, $N=32$ chunks, $B=10\text{MHz}$, $L=512$, subcarriers, 40-tap Rayleigh channel) 58

Figure 5.10: Sum rate of proposed algorithms (SNR=-5dB, $N=32$ chunks, $B=10\text{MHz}$, $L=512$, subcarriers, 60-tap Rayleigh channel) 58

Figure 5.11: PPAPR Analysis of proposed power allocation algorithm 60

SUM-RATE OPTIMAL RESOURCE ALLOCATION FOR SINGLE CARRIER FREQUENCY DIVISION MULTIPLE ACCESS SYSTEMS

SUMMARY

Wireless networks have been expanding very rapidly, and technology holders and researchers are challenged to develop new equipments and standardizations in wireless services, to fulfill this demand. The most crucial bottlenecks for the growth in wireless networks are the interference, multipath, transmitting power and available spectrum limitations. Multicarrier modulation technique is the outstanding solution over the 15 years to fulfill this consistently increasing demand. Orthogonal frequency division multiplexing (OFDM) deals with this multipath challenge by splitting whole bandwidth into smaller subcarriers, and then broadcasting them simultaneously. This approach reduces multipath distortion and reduces radio frequency (RF) interference so that the system has greater throughput. Orthogonal frequency division multiple access (OFDMA) is the multiple access scheme of OFDM. Although greater throughput of OFDMA system, it has a major drawback high peak-to-average-power ratio (PAPR). PAPR is a performance measurement that indicates the power efficiency of the OFDMA transmitter. If a signal has high PAPR, the OFDMA transmitter requires highly linear power amplifier to avoid excessive inter-modulation distortion. In order to avoid excessive inter-modulation between successive symbols, the power amplifier has to be operate with a large backoff from its peak power so that this linearity is achieved.

Single carrier frequency division multiple access (SC-FDMA) is a promising technique for uplink communications that require high data rate and has been adopted by 3rd generation partnership project (3GPP) for the current foremost cellular system, called long-term evolution (LTE). SC-FDMA is a modified form of OFDM, called as discrete Fourier transform (DFT)-spread orthogonal frequency multiplexing with similar throughput performance and complexity but lower PAPR. SC-FDMA transceiver has similar structure as a typical OFDM system except the addition of a DFT block before subcarrier mapping in the transmitter and a inverse-DFT (IDFT) after subcarrier de-mapping in the receiver. In other words, time-domain data symbols are transformed to frequency-domain by the DFT before going through the standard OFDM modulation. In addition, it uses frequency domain equalization, so it can easily mitigate inter-symbol interference (ISI).

The main advantage of SC-FDMA system is low PAPR of the transmit signal. PAPR is defined as the ratio of the peak power to average power of the transmit signal. From the point of view of mobile users, PAPR is the major concern, so low PAPR makes SC-FDMA system the preferred transmission technique for the uplink transmission. PAPR is mainly related to the power amplifier efficiency at the transmitter, and the

maximum power efficiency is obtained when the power amplifier is closely working at the saturation point. As SC-FDMA modulated signal can be viewed as a traditional single carrier signal because of its sequentially transmission, a pulse shaping filter can be applied to transmit signal to decrease PAPR due to OFDM.

In SC-FDMA systems, the subcarriers have to be grouped into subsets before being assigned to users. A set of particular subcarriers grouped together is called as chunk. There are two ways to map subcarriers to the user that are localized and distributed subcarrier mapping. In addition to this, if there is equidistant between the subcarriers in distributed subcarrier mapping, it is called interleaved subcarrier mapping. The subcarriers are adjacent to each other in localized subcarrier mapping and interleaved along to frequency in distributed subcarrier mapping. With no pulse shaping filters, interleaved SC-FDMA shows the best PAPR performance.

In radio environment, radio channels with wide bandwidth may experience frequency selective fading. This frequency selective nature of broadband channel transfer functions result channel dependent scheduling of pair of subcarriers and users. When users are dispersed spatially, each one has a different channel transfer function. Subcarrier assignment for different users have to be scheduled due to the channel conditions to increase total system throughput. Subcarriers are grouped in SC-FDMA systems, so it is called chunk assignment instead of subcarrier assignment. Besides, allocating total power of a user to the subcarriers of a selected chunk is also affecting total system throughput.

In this thesis, I obtained a jointly optimal power and chunk allocation policies which maximize the sum rate for a SC-FDMA system. The proposed solution is applicable to both localized and interleaved subcarrier mapping schemes. The joint optimization problem is solved by sequentially solving two sub-problems: power allocation and chunk allocation. Primarily, an optimal power allocation algorithm is used, which is derived from Karush-Kuhn-Tucker (KKT) conditions. The power allocation algorithm can be assumed as waterfilling in OFDM but it is a bit different from OFDM because an equalizer exists at the receiver. Then, the optimum chunk assignment problem is converted into a maximum weighted matching problem on a bipartite graph, and hence is solved it in polynomial time. Two greedy chunk allocation algorithms with lower complexity are also proposed: jointly greedy user-chunk allocation algorithm and greedy user allocation algorithm. Furthermore, it is demonstrated that these algorithms produce near optimal results, especially for interleaved subcarrier mapping for a channel with lower memory and both of interleaved and localized subcarrier mapping for a channel with higher channel memory, when used in conjunction with optimal power control.

TEK TAŞIYICILI FREKANS BÖLMELİ ÇOKLU ERİŞİM SİSTEMLERİ İÇİN TOPLAM VERİ HIZINI ENBÜYÜKLEYEN ÖZKAYNAK TAHSİSİ

ÖZET

Kablosuz ağlar günümüzde çok hızlı bir şekilde büyümektedir ve kablosuz ağları kullanım isteği de hızla artmaktadır. Hızla artan bu isteği karşılamak için, teknoloji üreticileri ve araştırmacılar yeni ekipmanlar, teknikler ve yöntemler geliştirip kablosuz servislerin standartlarını belirlerler. Kablosuz ağların gelişmesinde en can alıcı engeller interferans, çok yönlü yayılma, yayılan güç ve spektrum kısıtlamalarıdır. Spektrum, kablosuz ağlarda en değerli varlıktır ve geliştirilmesi mümkün değildir. Yayılan gücü arttırmak yerine, gücün verimli kullanılması esas alınmıştır. Çok-yönlü yayılmayı etkisiz kılmak için çok taşıyıcılı modülasyon tekniği ortaya atılmıştır. Çok taşıyıcılı modülasyon tekniği, sürekli ve hızla artan bu isteği karşılamak için önerilmiş can alıcı bir çözümdür. Dik frekans bölmeli çoğullama (OFDM) bu çok yönlü yayılım sorununu geniş bantlı küçük alt-taşıyıcılara bölerek ve sonrasında eşzamanlı ileterek üstesinden gelmiştir. Çok taşıyıcılı modülasyon tekniği çok yönlü yayılımı nedeniyle oluşan bozulmaları ve radyo frekans (RF) girişimini azaltır. Bu sayede yüksek miktarda işlem hacmine izin verir. Dik frekans bölmeli çoklu erişim (OFDMA) OFDM'in çoklu erişim tekniğidir. Üçüncü nesil mobil iletişim ortaklık projesi (3GPP), OFDMA'yi long-term evolution (LTE) sisteminde aşağı yönlü iletim için seçmiştir. OFDMA sistemi yüksek hızlarda işlem hacmine sahip olmasına rağmen, önemli bir sorun olan yüksek tepe-ortalama güç oranına (PAPR) sahiptir. PAPR, OFDMA göndericisinin güç verimliliğini belirten bir performans ölçümüdür. Mobil cihazlar için en önemli parametrelerde birisi cihazın güç verimliliğidir. Cihazın sahip olduğu güç, en verimli şekilde kullanılmalıdır. Eğer bir sinyal yüksek PAPR'a sahipse, intermodülasyon bozulmalarını engellemek için OFDMA göndericisi yüksek lineer bölgeyi güç yükselticisine gereksinim duyar. Ardışık semboller arasındaki bu aşırı aramodülasyon bozulmalarını engellemek için, güç yükselticisindeki bu lineerlik elde edilebilir diye güç yükseltici geniş gerçekleme ile çalıştırılmalıdır.

OFDM'de alt taşıyıcılar aynı anda paralel olarak iletilirler, bu nedenle PAPR değeri oldukça yüksektir. Bu sorunu çözebilmek için alt-taşıyıcıların paralel bir biçimde eşzamanlı olarak iletilmesi yerine ard arda iletilmesi ortaya atılmıştır. Bu sayede harcanan tepe gücün ortalama güce oranı OFDM'e göre düşük olacaktır. Fakat alt-taşıyıcıları ard arda iletmek için çok hızlı iletim yapmak gerekir ve bunun sonucunda da semboller arası girişim (ISI) meydana gelir. ISI'yı azaltmak için alıcıda denkleştirme yapılmalıdır. Denkleştirme sayesinde radyo kanalının çok-yönlü yayılma nedeniyle oluşan lineer bozulmaları telafi edilebilir. Genişband kanallar için kanal yanıt cevabı çok uzun olduğundan, geleneksel zaman bölgesi denkleştiriciler yerine frekans bölgesi denkleştiriciler alıcıda kullanılmalıdır. Tek taşıyıcılı frekans bölmeli çoklu erişim (SC-FDMA), yukarı yönlü yüksek data hızlarında iletim için umut verici bir yöntemdir ve 3GPP tarafından LTE'nin yukarı yönlü iletimine adapte edilmiştir.

Çünkü pil tüketimi mobil cihazlar için önemlidir ve alıcı kısım baz istasyonu olduğu için denkleştirici karmaşıklığı ve maliyeti gözardı edilebilir.

SC-FDMA, ayrık Fourier transform (DFT)-yayılmış dik frekans çoğullama olarak adlandırılan OFDM'in değiştirilmiş bir formudur. OFDM ile aynı işlem hacmi performansına ve karmaşıklığa, fakat düşük PAPR'a sahiptir. SC-FDMA alıcı-vericisi, tipik bir OFDM sistemiyle, vericideki alt-taşıyıcı eşlemeden önce eklenen DFT bloğu ve alıcıdaki alt-taşıyıcı ayırma işleminden sonra eklenen ters-DFT (IDFT) bloğu dışında tamamıyla aynıdır. Başka bir ifadeyle, zaman bölgesindeki bilgi sembolleri standart OFDM modülasyonundan önce DFT işlemiyle frekans bölgesine transfer edilir. Ayrıca, frekans bölgesi denkleştiricisi kullandığı için ISI'yı kolaylıkla azaltabilir.

SC-FDMA sisteminin OFDMA'e göre en önemli avantajı düşük tepe-ortalama güç oranına sahip olmasıdır. PAPR, vericideki güç yükselteciyle alakalıdır ve maksimum güç verimliliği, güç yükseltecinin doyum bölgesine yakın noktalarda çalışmasıyla elde edilir. SC-FDMA sistemiyle modüle edilmiş bir sinyal, klasik tek taşıyıcılı bir sinyal olarak gösterilebilir. Ayrıca sinyale darbe düzenleyici filtreler uygulanarak PAPR değerinin düşmesi sağlanabilir.

SC-FDMA sistemlerinde, sistemin yapısı gereği alt-taşıyıcılar kullanıcılara atanmadan önce gruplanmalıdır. Belirli alt-taşıyıcıların oluşturmuş olduğu küme "alt-taşıyıcı kümesi" olarak adlandırılır. Alt-taşıyıcıları gruplamanın iki temel yöntemi vardır: lokalize ve dağıtılmış alt-taşıyıcı eşleme. Buna ek olarak eğer dağıtılmış alt-taşıyıcı eşlemede alt-taşıyıcıların arasında eşit mesafe mevcut ise serpiştirilmiş alt-taşıyıcı eşleme olarak da adlandırılır. Lokalize alt-taşıyıcı eşlemede kümenin alt-taşıyıcıları birbirine bitişik olarak alınır. Serpiştirilmiş alt-taşıyıcı eşlemede ise kümenin alt-taşıyıcıları bütün frekans bandına yayılmış şekilde seçilir. Darbe şekillendirmenin olmadığı durumda, serpiştirilmiş alt-taşıyıcı eşlemede SC-FDMA sistemi en iyi PAPR performansını gösterir. Ayrıca serpiştirilmiş ve dağıtılmış alt-taşıyıcı eşleme frekans seçimi sönümlemeye karşı daha dayanıklıdır, çünkü gönderilecek olan bilgi mesajı bütün kanala yayılmıştır ve ardışık alt-taşıyıcılar üzerinde oluşabilecek olası derin sönümlenmelerden minimum düzeyde etkilenecektir. Diğer bir ifadeyle, dağıtılmış ve serpiştirilmiş alt-taşıyıcı eşleme frekans çeşitliliği sağlamaktadır. Lokalize alt-taşıyıcı eşleme ise alt-taşıyıcıları ardışık olarak seçtiğinden kanalda oluşabilecek olası derin sönümlenmelerden fazlasıyla etkilenecektir; fakat frekans seçici sönümleme nedeniyle alt-taşıyıcı kümelerine atanan kullanıcılar arasında kullanıcı çeşitliliği sağlayacaktır.

Radyo ortamında genişbandlı radyo kanalları frekans seçici sönümlemeye maruz kalırlar. Genişband kanal transfer fonksiyonlarının bu tarz bir sönümlemeye uğramalarının sonucu olarak kullanıcı alt-taşıyıcı çiftinin kanala bağlı atanması yapılmalıdır. Örneğin birden fazla kullanıcının olduğu bir çok taşıyıcılı sistemde, kullanıcılar baz istasyonundan uzaysal olarak ayrı konumlanmışlarsa, kullanıcıların her biri farklı bir kanal transfer fonksiyonuna sahip olacaktır. Bu nedenle sistemin toplam işlem hacmini arttırabilmek için alt-taşıyıcılar, kullanıcılara kanal durumları gözönünde bulundurularak atanmalıdır. Buna ek olarak, SC-FDMA sistemlerinde alt-taşıyıcılar kümeler halinde bulunduğundan alt-taşıyıcı ataması yerine "alt-taşıyıcı kümesi ataması" ifadesi kullanılır.

Mobil kullanıcıların batarya kısıtlamaları nedeniyle güç tüketimleri önemli bir parametredir ve gücün en optimal şekilde kullanılması istenir. Çok taşıyıcı bir sistem olan OFDMA'de mobil cihazlardaki mevcut gücün en optimal şekilde alt-taşıyıcılara aktarılması literatürde yıllardır fazlasıyla yer bulmuştur. Kullanıcının sahip olduğu toplam güç, kullanıcıya atanan alt-taşıyıcılara toplam işlem hacmini maksimize edecek şekilde paylaşılmalıdır. SC-FDMA sistemi içinde mevcut gücün paylaşılma şekli sistemin toplam işlem hacmini etkileyen en önemli parametrelerden birisidir. SC-FDMA'de alt-taşıyıcı kümesi kavramı ve alıcıda frekans bölgesi denkleştirici olmasına rağmen, mantık olarak güç paylaşırma OFDMA sistemindekine benzer biçimde yapılmaktadır.

Toplam işlem hacmini maksimize etmek için hem optimal alt-taşıyıcı kümesinin seçilmesi ve hem de kullanıcının mevcut gücünün alt-taşıyıcı kümesinin alt-taşıyıcılarına optimal biçimde aktarılması gerekmektedir. Bu durum iç içe bağlanmış bir sorundur ve çözülmesi oldukça karmaşıktır. Bu tezde SC-FDMA sisteminde toplam veri hızını maksimize eden birleşik optimal güç ve alt-taşıyıcı atama teknikleri elde edilmiştir. Elde edilen çözüm hem lokalize hem de serpiştirilmiş (dağıtılmış) alt-taşıyıcı atama için uygulanabilir. Birleşik optimizasyon problemi ardışık olarak iki alt problemin çözümüyle çözülmüştür: güç atama ve alt-taşıyıcı kümesi atama. Öncelikle, bir kullanıcı herhangi bir alt-taşıyıcı kümesi seçtikten sonra, o alt-taşıyıcı kümesinin elemanlarına mevcut gücünü optimal bir şekilde paylaşmaktadır. Güç paylaşırma bir iç bükey optimizasyon problemidir ve Karush-Kuhn-Tucker (KKT) koşullarından türetilen bir güç paylaşırma algoritmasıyla çözülmüştür. Güç paylaşırma algoritması, OFDM'deki su doldurma algoritması gibi düşünülebilir ama SC-FDMA alıcısında bulunan frekans bölgesi denkleştiricisi nedeniyle elde edilen fonksiyon OFDM'de elde edilenden farklıdır. Önerilen güç paylaşırma algoritmasının zaman karmaşıklığı en kötü durumda $O(M \log M)$ olarak hesaplanmıştır (M : bir alt taşıyıcı kümesinin sahip olduğu alt-taşıyıcı sayısı). SC-FDMA sistemlerinde $M=12$ alt-taşıyıcı olarak belirlendiğinden, bu algoritma oldukça kısa sürede yakınsamaktadır.

Bütün kullanıcılar sistemde bulunan bütün alt-taşıyıcı kümelerine güç paylaşırmasını denedikten sonra alt problemlerden ikincisi olan optimal alt-taşıyıcı kümesi atama problemi devreye girer. Optimal alt-taşıyıcı kümesi atama problemi iki taraflı grafik üzerinde maksimum ağırlıklı eşleme problemine dönüştürülmüş ve Hungarian algoritması ile polinomsal zamanda çözülmüştür. Bu algoritmanın zaman karmaşıklığı $O(\max(N, K)^3)$ olarak hesaplanmıştır (N : alt-taşıyıcı kümesi sayısı, K : toplam kullanıcı sayısı). Alt-taşıyıcı kümesi atama probleminin optimal çözümünün zaman karmaşıklığı oldukça uzun olduğundan, zaman karmaşıklığı kısa ama optimal çözüme yakın sonuçlar veren iki açgözlü alt-taşıyıcı atama algoritması önerilmiştir: birleşik Açgözlü kullanıcı-alt-taşıyıcı kümesi atama algoritması ve açgözlü kullanıcı atama algoritması. İlk algoritmanın zaman karmaşıklığı $O(N^2K)$ olarak bulunmuştur. Genellikle kullanıcı sayısı, alt-taşıyıcı kümesi sayısından fazla olduğundan ($N < K$) optimal çözüme göre daha kısa sürede bitmektedir. İkinci önerilen algoritmanın zaman karmaşıklığı ise $O(NK)$ olarak hesaplanmıştır ve optimal çözüme göre oldukça kısa sürede bitmektedir. İki algoritma da optimal çözüme göre kısa sürede bitmesine rağmen performans bakımından yaklaşık olarak optimal sonucu vermişlerdir.

Yapılan simülasyonlar sonucunda bir optimal ve optimal olmayan iki algoritmanın performansları incelenmiştir. Optimal olmayan iki algoritma zaman karmaşıklığı optimale göre kısa olmasına rağmen performans olarak optimale yakın sonuçlar vermiştir. Önerilen bütün algoritmalar hem lokalize hem de serpiştirilmiş alt-taşıyıcı atama için geçerlidir. Özellikle kanal hafızasının düşük olduğu radyo kanallarında serpiştirilmiş alt-taşıyıcı kümesi atamasında optimale yakın sonuçlar elde edilmiştir, kanal hafızasının yüksek olduğu radyo kanallarında ise her iki alt-taşıyıcı atama için de optimale yakın sonuçlar elde edilmiştir. Kanal hafızasının düşük olduğu radyo kanallarda, güç paylaşırma algoritması serpiştirilmiş alt-taşıyıcı atama için anlamlı haldedir.

Yapılan bu çalışmada, birleşik güç ve alt-taşıyıcı atama için önerilen algoritmalarda her kullanıcıya bir tane alt-taşıyıcı kümesi verilmiştir. Gelecekte yapılacak çalışmalarda, kullanıcılara birden fazla alt-taşıyıcı kümesi verilmesi durumu incelenmelidir. Bu tümleşik bir problemdir; çünkü tek bir kullanıcı için bile birden fazla alt-taşıyıcı kümesi atandığında iki sorun göze çarpmaktadır: hangi alt-taşıyıcı kümeleri seçilecek ve seçilen bu kümelere kullanıcının gücü nasıl paylaşılacak? Bu soruların cevapları bulunarak bu çalışma geliştirilebilir. Ayrıca zaman karmaşıklığı daha kısa optimal olmayan alt-taşıyıcı kümesi atama algoritmaları bulunabilir.

1. INTRODUCTION

High-rate data communications are severely affected by intersymbol interference (ISI) caused by the natural time delay of the wireless channel. One powerful way of mitigating ISI is the use of multicarrier modulation techniques, the most popular of which is orthogonal frequency division multiplexing (OFDM). The orthogonal nature of OFDM also enables its use as a multiple accessing technique, which is called orthogonal frequency division multiple access (OFDMA). However, it is now well known that OFDMA systems have a major drawback, as they suffer from high peak-to-average power ratio (PAPR). High PAPR is undesired especially in the uplink, as portable devices that are trying to communicate with base station consume much power in an OFDMA uplink system, and they have to have a radio frequency (RF) power amplifier that has a wide linear range and is therefore more expensive than traditional RF power amplifiers [1].

Single carrier frequency division multiple access (SC-FDMA) is becoming an increasingly popular choice for uplink transmissions, thanks to its ability to resolve the high peak to average power ratio issue commonly faced in OFDMA systems [2,3]. As a result, it has now entered the standards, such as long term evolution (LTE)-Advanced, and efficient resource allocation for SC-FDMA therefore remains a hot topic.

A SC-FDMA system can be considered as a pre-coded OFDMA system, whose data signals are pre-coded by a discrete Fourier transform (DFT) block before subcarrier mapping at the transmitter, and decoded by an inverse DFT (IDFT) block after subcarrier de-mapping at the receiver [2]. In SC-FDMA, the subcarriers have to be grouped into sets before being assigned to users. A set of particular subcarriers grouped together is called a chunk. While pre-coding and use of chunks reduce the PAPR compared to the OFDMA system, the ISI rejection capability is reduced and the SC-FDMA system needs to use frequency domain equalizers to mitigate ISI [4].

1.1 Literature Review

The resource allocation problem for OFDMA systems has been extensively studied in the literature. A transmit power adaptation method that maximizes the total data rate of multiuser OFDM systems in a downlink transmission was proposed in [5]. A joint subcarrier and power allocation problem with the objective of maximizing the total utility of users in the uplink of an OFDMA system was proposed in [6]. A low-complexity suboptimal algorithm that separates subchannel allocation and power allocation regarding proportional rate constraints for multi-user OFDMA system is proposed in [7]. In [8], they derived a multiuser convex optimization problem to find the optimal allocation of subchannels, and proposed a low-complexity adaptive subchannel allocation algorithm for multi-user OFDM system. Subcarrier, power, and rate allocation schemes for the OFDMA uplink were considered and a low-complexity algorithm with fairness consideration was proposed to maximize the sum rate under individual rate and transmit power constraints in [9]. A joint subcarrier and power allocation in uplink OFDMA systems with incomplete channel state information was proposed in [10]. In addition, the subcarrier allocation problem was also considered as a multi-player discrete, stochastic and finite strategy game, and equal power was allocated to the subcarriers of each user in [10]. The problem of joint subcarriers and power allocation for the downlink of a multi-user multi-cell OFDM cellular network in [11]. They developed a distributed solution to find the globally optimal allocation which determines the subcarrier and power allocation dynamically and investigated the impact of reducing the complexity by reducing the number of degrees of freedom available in the optimization. The joint subcarrier and power allocation problem with the objective of maximizing the total utility of users in the uplink of an OFDMA system was also considered in [12]. Their formulation included the problems of sum rate maximization, proportional fairness and max-min fairness as special cases. A multiuser OFDM subcarrier, bit, and power allocation algorithm to minimize the total transmit power was proposed by assigning each user a set of subcarriers and by determining the number of bits and the transmit power level for each subcarrier in [13]. Basestation allocation of subcarriers and power to each user was considered to maximize the sum of user data rates, subject to constraints on total

power, bit error rate, and proportionality among user data rates in [14]. In [15], subcarrier and power allocation in multiuser OFDM was considered to maximize the overall rate while achieving proportional fairness amongst users under a total power constraint. In addition, specifically, a multiuser orthogonal frequency-division multiplexing subcarrier, bit and power allocation algorithm to minimize the total transmit power was proposed by assigning each user a set of subcarriers and by determining the number of bits and the transmit power level for each subcarrier in [16]. An optimal joint subcarrier and power allocation algorithm for OFDMA systems was proposed in [17].

The joint resource allocation problem for SC-FDMA, however, has a considerably different nature than that for an OFDMA system, due to the inherent requirement that the subcarriers have to be grouped into chunks. As a result, the works on resource allocation for SC-FDMA have almost invariably focused on chunk allocation only. The problem of chunk allocation for the uplink of an SC-FDMA system with a minimum mean square error (MMSE) equalizer was considered in [4], the impact of imperfect channel state information (CSI) on channel dependent scheduling of SC-FDMA system in [18] and a proportional fair scheduling was proposed in [19]. Yet, power allocation was not employed in [4], which assigned equal powers to all subcarriers in the same chunk and proposed greedy algorithms for chunk allocation. An optimal solution, as well as a greedy algorithm for resource allocation in uplink SC-FDMA systems were proposed in [20], without considering power allocation. In [21], the greedy solution provided in [20] was improved and three algorithms based on greedy approaches were developed: weighted sum-rate maximization, transmission with minimal number of subchannels and sum-power minimization. However, joint optimization of chunks and powers was not carried out. The solution of [4] was improved by swapping pairs of users assigned by a greedy algorithm in [22]. In [23], another modification of the greedy algorithm of [4], called maximum greedy algorithm was proposed. In [24], a virtual multiple input multiple output (V-MIMO) model was used and assuming that two users transmit their data in the same time slot and frequency band, a combination of the Hungarian algorithm and the binary switching algorithm for chunk allocation was proposed. In addition, the impact of radio resource

allocation and pulse shaping on the PAPR of SC-FDMA signals were investigated, especially for localized FDMA (LFDMA) signals in [25]. The resource allocation problem for SC-FDMA systems in LTE uplink in [26]. The resource allocation problem was first formulated and a heuristic algorithm further proposed to find feasible solution to the problem.

1.2 Purpose of the Thesis

Unlike the previous works on resource allocation for SC-FDMA that focus only on chunk allocation without power allocation, or vice-versa, In this thesis, we focused on joint allocation of chunks and transmit powers for uplink SC-FDMA systems, and proposed a jointly optimal power and chunk allocation algorithm. First, the problem is separated into two sub-problems: optimal power allocation and optimal chunk allocation. Primarily, the power allocation algorithm, which is derived from the Karush Kuhn Tucker (KKT) conditions, assigns the power of each of the users, to the subcarriers of each given chunk, thereby determining the rate achievable by each user on each chunk. Then a maximum weighted matching algorithm finds the matching between the users and chunks which maximizes the total rate of the system. Finally, two greedy algorithms for joint chunk and power allocation to maximize the overall sum rate are proposed.

1.3 Preview of the Thesis

In the first chapter, motivation of the thesis, literature review related to the subject of the thesis and the purpose of the thesis are presented. The rest of the thesis is organized as follows. In Chapter 2, channel characteristics of wireless channels, capacity and Gaussian channel and optimization problems are presented. In chapter 3, detailed information about frequency multiplexing and single carrier FDMA are presented. In Chapter 4, sum-rate optimal resource allocation problem is given and solved. Chapter 5 contains simulation results of the proposed solutions. Conclusion remarks and future work are given in Chapter 6.

2. BACKGROUND THEORY

2.1 Channel Characteristics

Radio signal propagation in cellular systems is one of the popular subject that investigating by researchers both theoretically and experimentally. The following subsections describe mobile radio propagation aspects briefly.

In wireless networks, receiver can not receive exact signal that is transmitted by transmitter. Random fluctuations occur in received signal amplitude in the receiver. These unwanted random fluctuations depend on relative speed, frequency (wavelength) or environment.

2.1.1 Transmit and receive signal models

Transmit and receive signal models have to be explained before the propagations models. Both of the signal models are considered as real. That is because modulators are built using oscillators that generates real sinusoids not complex components [27]. Real modulated and demodulated signals are often represented as a real part of a complex signal. For simplicity, bandpass signals are represented in complex baseband. Carrier frequency of a communication system, f_c , is much bigger than bandwidth of the system, B , ($f_c \gg B$) so that a system is bandpass system. In mobile communications systems, transmitted signal, $s(t)$, of a bandpass system is expressed as follow:

$$\begin{aligned} s(t) &= \Re\{u(t)e^{j2\pi f_c t}\} \\ &= \Re\{u(t)\} \cos(2\pi f_c t) - \Im\{u(t)\} \sin(2\pi f_c t) \\ &= x(t) \cos(2\pi f_c t) - y(t) \sin(2\pi f_c t), \end{aligned} \tag{2.1}$$

where the signal $u(t)$ is called complex envelope or complex lowpass equivalent signal of the transmitted signal $s(t)$. In addition, $u(t) = x(t) + jy(t)$ is a complex baseband signal with in-phase component $x(t) = \Re\{u(t)\}$ and quadrature component

$y(t) = \Im\{u(t)\}$. $u(t)$ is the complex envelope of $s(t)$ since magnitude and phase of $u(t)$ is equal to magnitude and phase of $s(t)$, respectively.

The received signal, $r(t)$, have similar form as transmitted signal:

$$r(t) = \Re\left\{v(t)e^{j2\pi f_c t}\right\}, \quad (2.2)$$

where $v(t)$ is the complex baseband signal which depends the transmitted signal, $s(t)$, and the channel parameters through $s(t)$ propagates [27].

2.1.2 Large scale propagation model

The purpose of the large scale propagation model is to predict received signal strength when transmitter and receiver have a clear, unobstructed line-of-sight (LOS) between them. Satellite systems, LOS microwave systems, etc. can be given as an example for this propagation model.

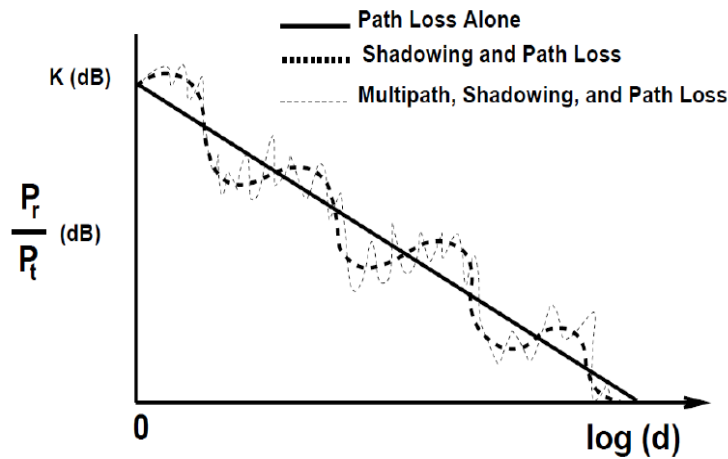


Figure 2.1: Multipath, shadowing and path loss versus distance [27].

2.1.2.1 Path loss

Free space propagation model need to be mentioned before path loss concept. Friis free space equation that is valid for far-field is used to determine the power received by one antenna under idealized conditions given another antenna some distance away transmitting a known amount of power. The received signal is inversely proportional to the square of the distance between the transmitter and receiver, and also inversely proportional to the square of the frequency of the radio signal.

$$P_r(d) = \frac{P_t G_t G_r \lambda^2}{(4\pi)^2 d^2 L}, \quad (2.3)$$

$P_r(d)$ - received signal strength at distance d ,

P_t - transmitted signal strength,

G_t - transmitter antenna gain,

G_r - receiver antenna gain,

λ - wavelength(m),

d - distance between transmitter and receiver(m),

L - system loss not related to propagation (≥ 1 ; No Loss Case $L = 1$).

Difference between effective transmit power at transmitter and received power at receiver is called path loss. Free space path loss can be express in dB as follows:

$$PL[dB] = 10\log_{10} \left(\frac{P_t}{P_r} \right) = 10\log_{10} \left(\frac{G_t G_r \lambda^2}{(4\pi)^2 d^2} \right). \quad (2.4)$$

In far-field region, the received signal strength is expressed as follows:

$$P_r(d) = P_r(d_0) \left(\frac{d_0}{d} \right)^2, \quad (2.5)$$

where d_0 is pre-defined distance between transmitter and receiver and $P_r(d_0)$ is pre-defined received signal strength.

2.1.2.2 Shadowing

The path loss in radio propagation model has been derived in Section 2.1.2.1 that is only effected by distance between transmitter and receiver and path loss exponent of the environment at where the transmitted signal propagates. Due to the path loss formula, the received signal strength would be same level at equally distance from the transmitter at same environment that has same path loss exponent. However, there is a noticeable variation in the strength of received signals at different points that are equidistance from the transmitter.

Figure 2.1 shows slow variations in the strength of the received signals that are represented by dashed line. These slow variations are called shadowing effect and would be caused by shadowing from terrain, buildings and trees.

Before stating definition of shadowing effect over a radio propagation model, definitions of basic Gaussian distribution, Q-function and Error Function (erf) have to be stated. These functions are generally used to indicate the probability that the received signal strength will exceed a particular level.

Gaussian probability distribution function, $f_x(x)$, is:

$$f_x(x) = \frac{1}{\sqrt{2\pi\sigma^2}} e^{-(x-\mu)^2/2\sigma^2}, \quad (2.6)$$

where x is random variable, σ and μ is standard deviation and mean of random variable, respectively.

Q-function and error function of zero mean unit variance Gaussian distribution are:

$$Q(z) = \frac{1}{\sqrt{2\pi}} \int_z^\infty e^{-x^2/2} dx = \frac{1}{2} \left[1 - \text{erf}(z/\sqrt{2}) \right]. \quad (2.7)$$

The shadowing effect of over a radio propagation model is added to path loss in dB [28]:

$$PL(d)[dB] = PL(d_0) + 10n \log_{10} \left(\frac{d}{d_0} \right) + X_\sigma, \quad (2.8)$$

where X_σ is zero-mean Gaussian distributed random variable with standard deviation σ in dB.

The probability that the received signal strength exceeds a certain value γ can be calculated from the cumulative density function as [28]:

$$Pr[P_r(d) > \gamma] = Q \left(\frac{\gamma - \bar{P}_r(d)}{\sigma} \right). \quad (2.9)$$

Similarly, the probability that the received signal strength is below a certain value γ which is also called outage probability:

$$Pr[P_r(d) < \gamma] = Q \left(\frac{\bar{P}_r(d) - \gamma}{\sigma} \right). \quad (2.10)$$

2.1.3 Small scale propagation model

Small scale propagation model is generally called as small scale fading or simply fading. Small scale fading is defined as unexpected changes in signal amplitude and phase that can be experienced as a result of small changes in the spatial separation between a receiver and transmitter. The type of small scale fading experienced by a signal propagating through a mobile radio channel depends on the nature of the transmitted signal with respect to the characteristics of the radio channel. The main factors influencing the small scale fading are mainly: multi path propagation, speed of mobile (mobile can be either transmitter or receiver or both of them), speed

of surrounding objects and transmission bandwidth of the channel as well as the bandwidth of the signal [28].

Small scale fading manifests itself in two mechanisms:

- Frequency-spreading of the signal: Generated by the motion between the transmitter and receiver and that results in the appearance of Doppler effect and so a parasitic frequency modulation. If the multiple reflective paths are large in number and there is no line-of-sight signal component, the different Doppler frequencies and amplitudes of each paths implies that the envelope of the received signal is statistically described by a Rayleigh probability density function. This time-variant manifestation of the fading can be categorized as fast or slow fading as explained in Section 2.1.3.2.
- Time-spreading of the signal: Generated by the multiple paths in the radio signal. Depending on the symbol duration with respect to this delay spread, frequency selective fading can appear and so signal distortion. This frequency-variant manifestation of the fading can be then categorized as frequency-selective or frequency-non-selective (flat), as further explained in Section 2.1.3.2.

2.1.3.1 Coherence time and bandwidth

Coherence time, T_c , is the period of time over in which the radio channel impulse response is considered to be not varying or time invariant. In other words, it can be stated as the period of time after which the correlation function of two samples of the channel response taken at the same frequency but different time instants drops below a predetermined threshold. Coherence time can be expressed in mathematically as inverse of maximum Doppler shift:

$$T_c \approx \frac{1}{f_{d_{max}}}. \quad (2.11)$$

Coherence bandwidth, B_c , is the statistical measure of the range of frequencies over which the channel can be considered flat. In other words, it is the range of frequencies over which two frequency components have a strong potential for amplitude correlation. The rms delay spread, σ_τ , and coherence bandwidths are

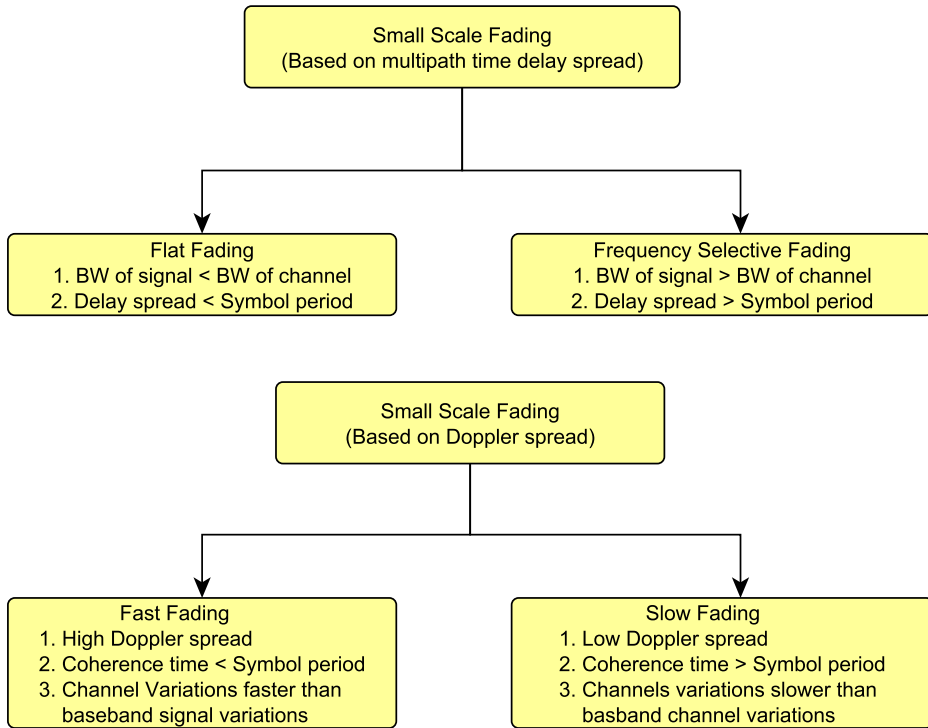


Figure 2.2: Types of small scale fading [28].

inversely proportional to each other:

$$B_c \propto \frac{1}{\sigma_\tau}. \quad (2.12)$$

Rms delay spread, σ_τ , is the square root of the second central moment of the power delay profile which is defined as:

$$\sigma_\tau = \sqrt{\tau^2 - (\bar{\tau}^2)}, \quad (2.13)$$

where τ is the time delay and $\bar{\tau}$ is mean excess delay which is the first moment of the power delay profile and defined as:

$$\bar{\tau} = \frac{\sum_n \alpha_n^2 \tau_n}{\sum_n \alpha_n^2}, \quad (2.14)$$

where α_n is the path attenuation factor [28].

2.1.3.2 Types of small scale fading

Small scale fading: slow fading vs. fast fading

The transmitter, receiver or many objects through the radio channel are likely to be moving, and as a result of this movement, the path lengths of all signals being received

are changing randomly. Depending of these variations in the transmitted baseband signal compared to the rate of the channel, a channel may be classified either as a fast fading or slow fading channel [28].

In a fast fading channel, the coherence time of the channel is smaller than the symbol period of the transmitted signal. Due to the Doppler effect, this causes frequency dispersion which leads to signal distortion. A signal undergoes fast fading if:

$$T_s \gg T_c, \quad (2.15)$$

in the time domain where T_s is the symbol period of the transmitted signal or similarly:

$$B_s \ll f_{d_{max}}, \quad (2.16)$$

in the frequency domain where B_s is the bandwidth of the transmitted signal.

In a slow fading channel, Doppler spread of the wireless channel is much less compared to the baseband bandwidth of the transmitted signal and coherence time of channel is greater than the transmitted signal symbol duration. A signal undergoes slow fading if:

$$T_s \ll T_c, \quad (2.17)$$

in the time domain or similarly:

$$B_s \gg f_{d_{max}}, \quad (2.18)$$

in the frequency domain.

Small scale fading: frequency-selective fading vs. flat fading

In a small scale fading channel, the relationship between rms delay spread of the channel σ_τ and the symbol period of the transmitted signal T_s characterize the signal dispersion. Depending of these two parameters, a channel may be either flat fading or frequency-selective fading channel.

If it has a constant gain and linear phase response over a bandwidth which is more than that of the transmitted signal, a channel is said to convey a *flat fading* effect. Flat fading channel has its multipath rms delay spread σ_τ much smaller than the transmitted signal symbol period T_s

$$\sigma_\tau \ll T_s, \quad (2.19)$$

and coherence bandwidth of the channel B_c is greater than bandwidth of the transmitted signal B_s

$$B_c \gg B_s. \quad (2.20)$$

As a result of this, flat fading channel affects all frequency components of a narrow band transmitted signal in the same way. Therefore, the signal will experience the same magnitude of fading at the receiver.

If a wireless channel has a constant gain and linear phase response over a bandwidth which is less than bandwidth of the transmitted signal, the channel will reflect frequency-selective fading or selective fading on the received signal. A signal undergoes frequency-selective fading channel if delay spread of the channel σ_τ is larger than the symbol period of the transmitted signal T_s :

$$\sigma_\tau > T_s, \quad (2.21)$$

and similarly, a signal undergoes frequency-selective fading channel if coherence bandwidth of the channel B_c is much smaller than bandwidth of the transmitted signal B_s :

$$B_s > B_c. \quad (2.22)$$

As a result of the frequency-selective fading, the different frequency components of the signal therefore experience uncorrelated fading.

In addition, a common rule is accepted by everyone a channel is flat fading if $T_s \geq 10\sigma_\tau$ and a channel is frequency selective if $T_s < 10\sigma_\tau$ although this is dependent on the specific type of modulation used [28].

2.2 Capacity and Gaussian Channel

Claude E. Shannon presented his seminar work "A Mathematical Theory of Communication" in 1948 and pioneered to the modern digital communication as understood nowadays. He developed his theory to find fundamental boundaries on signal processing operations such as compressing data, storing and communicating data reliably. Transmitting of information over a noisy channel is the primary paradigm of classical information theory that was investigated by searchers. Shannon's source

coding theorem is the most fundamental and leading theory that establishes that the number bits, on average, needed to represent the result of an uncertain event is given by its entropy. In addition to this, Shannon's coding of noisy channel theorem states that reliable communication is possible over noisy channels provided that the rate of communication is below a certain threshold, which called as channel capacity [29].

The simplest and best model for channel model is the additive white Gaussian noise (AWGN) channel that is a special case of Gaussian channel to communicate point-to-point channel.

In such a channel, the output, denoted by Y , is equal to the sum of the input x and additive Gaussian noise N as shown in Figure 2.3:

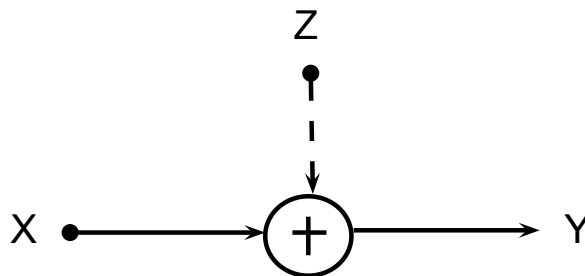


Figure 2.3: Gaussian channel.

In general form of the Gaussian channel in mathematically:

$$Y_i = X_i + Z_i, \quad (2.23)$$

where X_i and Y_i is the channel input and output, respectively and Z_i is zero mean Gaussian random variable with N variance: $Z_i \sim \mathcal{N}(0, N)$. The noise Z_i is assumed to be independent of the input signal X_i . This channel model valid for some common communication channels, such as wired and wireless fixed phone and satellite links. If the noise variance of the channel is zero, the receiver receives only the transmitted symbol then the channel capacity of this channel may be infinite in theory.

It is also assumed that there is a constraint on transmitting power, such that if we have a input codeword (x_1, x_2, \dots, x_n) , the average power P is constrained to:

$$\frac{1}{n} \sum_{i=1}^n P_i \leq P \quad (2.24)$$

To analyse this channel a simple suboptimal way can be used. Assume that only one bit is transmitted on this channel (either 1 or 0), called binary transmission. Considering

the probability error for binary transmission, the power of transmitted power can be either $-\sqrt{P}$ or $+\sqrt{P}$ over the Gaussian channel. Both of the levels are assumed that equally likely, the optimum decoding rule is to decide that $+\sqrt{P}$ if $Y > 0$ and $-\sqrt{P}$ if $Y < 0$, so the receiver detects the signal and decodes it according to the envelope amplitude of the signal such that:

$$\begin{aligned}
P_e &= \frac{1}{2}P(Y < 0|X = \sqrt{P}) + \frac{1}{2}P(Y > 0|X = -\sqrt{P}) \\
&= \frac{1}{2}P(Z < -\sqrt{P}|X = \sqrt{P}) + \frac{1}{2}P(Z > \sqrt{P}|X = -\sqrt{P}) \\
&= P(Z > \sqrt{P}) \\
&= \int_{\sqrt{P}}^{\infty} \frac{1}{\sqrt{P} \sqrt{2\pi N}} e^{-\frac{x^2}{2N}} dx \\
&= Q(\sqrt{P/N}) = 1 - \Phi(\sqrt{P/N}), \tag{2.25}
\end{aligned}$$

where $\Phi(x)$ is the cumulative normal function:

$$\Phi(x) = \int_{-\infty}^x \frac{1}{\sqrt{2\pi}} e^{-\frac{t^2}{2}} dt. \tag{2.26}$$

The information capacity of the Gaussian channel under the assumption derived in (2.25):

$$C = \max_{p(x):E[X^2] \leq P} I(X;Y). \tag{2.27}$$

Entropy of this formula is calculated as follows:

$$\begin{aligned}
I(X;Y) &= h(Y) - h(Y|X) \\
&= h(Y) - h(X + Z|X) \\
&= h(Y) - h(Z) \\
&\leq \frac{1}{2} \log 2\pi e(P + N) - \frac{1}{2} \log 2\pi eN \\
&= \frac{1}{2} \log(1 + P/N) \quad \text{bits/transmission.} \tag{2.28}
\end{aligned}$$

The capacity of a Gaussian channel with power constraint P and noise variance N is derived in (2.28). Channel capacity of a bandlimited channel is considered in the following section.

2.2.1 Capacity of a bandlimited channel

A basic model for a communication over a radio link or a fixed line telephone is a bandlimited channel with white noise. This is a continuous time channel and the output is described as the convolution of sum of input signal and noise component.

$$Y(t) = (X(t) + Z(t)) * h(t), \quad (2.29)$$

where $X(t)$ is the input signal waveform varying with time, $Z(t)$ is the waveform of the where Gaussian noise and $h(t)$ is the impulse response of an ideal bandpass filter that has a bandwidth of W Hz.

Definition: The function $h(t)$ is bandlimited to W , namely, the spectrum of the function is 0 for all frequencies greater than W . In addition, the function is completely determined by samples of the function spaced at least $\frac{1}{2W}$ that is known as Nyquist sampling Theorem [29].

The noise is white and Gaussian and assumed each component is independent, identically distributed (IID) Gaussian random variable. Furthermore, it has power spectral density $N_0/2$ Watts/Hertz and bandwidth W Hertz, so the noise has $\frac{N_0}{2}2W = N_0W$. In each time interval T , the noise has $2WT$ samples and variance $N_0WT/2WT = N_0/2$.

The channel capacity of a Gaussian channel is derived in (2.28). The energy per sample is $PT/2WT = P/2W$ and the noise variance per sample is $\frac{N_0}{2}2W \frac{T}{2WT} = N_0/2$ in time interval T . Consequently, the channel capacity of a Gaussian channel becomes:

$$C = \frac{1}{2} \log \left(\frac{1 + \frac{P}{2W}}{\frac{N_0}{2}} \right) = \frac{1}{2} \log \left(1 + \frac{P}{N_0W} \right) \text{ bits/sample.} \quad (2.30)$$

Since there is $2W$ samples in each second, the channel capacity can be rewritten as:

$$C = W \log \left(1 + \frac{P}{N_0W} \right) \text{ bits/second.} \quad (2.31)$$

This is the most well-known and famous formula of information theory. It gives the channel capacity of a bandlimited Gaussian channel with power P and noise spectral density $N_0/2$ Watts/Hz [29].

2.2.2 Parallel Gaussian channel

Before the consideration of parallel Gaussian channel, Nonlinear Optimization and KKT condition have to be mentioned. It is particularly considered in Section 2.3.

Consider k independent Gaussian channels in parallel with a common power constraint P . The objective is to allocate the total power among the channels so that the channel capacity is maximized. The noise is not white Gaussian and each parallel component represents a different frequency. The output of channel j as shown in Figure 2.3:

$$Y_j = X_j + Z_j, \quad j = 1, 2, \dots, k, \quad (2.32)$$

where $Z_i \sim \mathcal{N}(0, N)$ and assumed to be independent from channel to channel.

Assume a constraint on total power extending the constraint derived in Section 2.2

$$E \left[\sum_{j=1}^k X_j^2 \right] \leq P. \quad (2.33)$$

The information capacity of the parallel Gaussian channel is:

$$\begin{aligned} I(X_1, \dots, X_k; Y_1, \dots, Y_k) &= h(Y_1, \dots, Y_k) - h(Y_1, \dots, Y_k | X_1, \dots, X_k) \\ &= h(Y_1, \dots, Y_k) - h(Z_1, \dots, Z_k) \\ &= h(Y_1, \dots, Y_k) - \sum_{i=1}^k h(Z_i) \\ &\leq \sum_{i=1}^k h(Y_i) - h(Z_i) \\ &\leq \sum_i \frac{1}{2} \log(1 + P_i/N_i). \end{aligned} \quad (2.34)$$

From (2.34), it can be say that the allocation of powers for each parallel channel is reasonably selected so that the channel capacity is maximum. The power constraint is based on Lagrangian operation and becomes as follows:

$$J(P_1, P_2, \dots, P_k) = \sum_i \frac{1}{2} \log \left(1 + \frac{P_i}{N_i} \right) + \lambda \sum_i P_i, \quad (2.35)$$

with a constraint that $P_i \geq 0$. Differentiating with respect to P_i

$$\frac{1}{2} \frac{1}{P_j + N_j} + \lambda \geq 0. \quad (2.36)$$

In addition, (2.36) becomes equality if and only if all constraints are inactive, i.e. $\lambda = 0$. After some trivial mathematical manipulations, (2.36) can be rewritten as:

$$P_j = v - N_j. \quad (2.37)$$

However, since the P_i 's must be nonnegative, it may not always be possible to find a solution of this form. In such a case, KKT conditions are used to verify that solution. Thus, it has to be ensured that $N_j < v$. Let

$$P_j = (v - N_j)^+, \quad (2.38)$$

where

$$(x)^+ = \begin{cases} x, & x \geq 0 \\ 0, & x < 0 \end{cases} \quad (2.39)$$

and v is chosen so that

$$\sum_{i=1}^n (v - N_i)^+ = P. \quad (2.40)$$

This solution is illustrated in Figure 2.4. The vertical levels show the noise power for various parallel channels. The power that is allocated to a channel is inversely proportional to the noise level of the channel, so it can be said that less power is allocated to noisier channels. This process is similar to the way in which water distributes itself in a vessel, so this process is referred to as waterfilling. Besides, in Figure 2.4, v is called as water level for these parallel Gaussian channels.

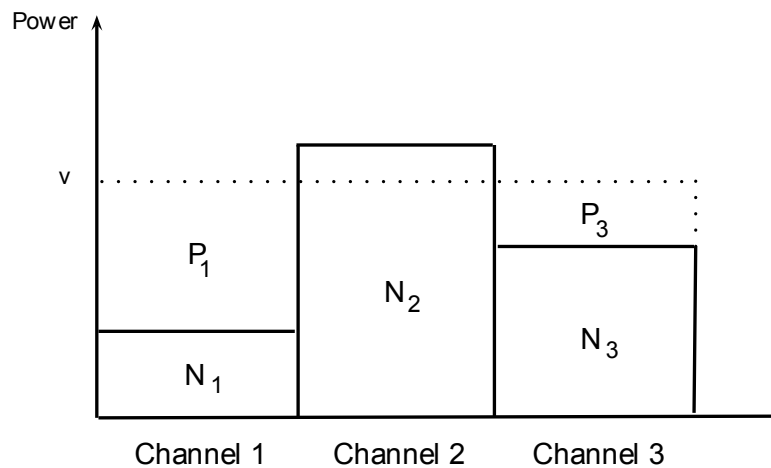


Figure 2.4: Waterfilling technique for parallel channels.

2.3 Optimization Problems

Allocation of powers to the parallel Gaussian channels is a optimization problem. The power has to be allocated to the parallel channels in a way that channel capacity is maximum described in Section 2.2.2.

For an optimization problem, the following terminology is used:

$$\begin{aligned} &\text{minimize} && f_0(x) \\ &\text{subject to} && f_i(x) \leq 0, \quad i = 1, \dots, m \\ &&& h_i(x) = 0, \quad i = 1, \dots, p \end{aligned} \tag{2.41}$$

where x is the optimization variable, $f(\cdot)$ is the objective or cost function, $f_i(\cdot)$, ($i = 1, \dots, m$) are the inequality constraint functions, and $h_i(\cdot)$, ($i = 1, \dots, p$) are the equality constraint functions. The number of inequality and equality constraints are denoted m and p , respectively [30].

The optimization problem is generally expresses as a minimization problem; but it can also be a maximization problem:

$$\begin{aligned} &\text{maximize} && f_0(x) \\ &\text{subject to} && f_i(x) \leq 0, \quad i = 1, \dots, m \\ &&& h_i(x) = 0, \quad i = 1, \dots, p \end{aligned} \tag{2.42}$$

by minimizing the function $-f_0$ subject to the constraints.

2.3.1 Convex optimization problems

Convex optimization problems are one of the particular form of the optimization problem and also called as nonlinear programming. A convex optimization problem:

$$\begin{aligned} &\text{minimize} && f_0(x) \\ &\text{subject to} && f_i(x) \leq 0, \quad i = 1, \dots, m \\ &&& a_i^T x = b_i, \quad i = 1, \dots, p \end{aligned} \tag{2.43}$$

where f_0, \dots, f_m are convex functions. The convex optimization problem is different from the traditional optimization problem with the following requirements:

- the cost function must be convex,
- the inequality functions must be convex,
- the equality constraint functions $h_i(x) = a_i^T x - b_i$ must be affine.

2.3.2 Concave maximization problems

The optimization problems can also be a concave maximization problem that is one of the main subject of this thesis. The power allocation in a pre-defined chunk (a set of subcarriers) is a concave maximization problem. It is referred to:

$$\begin{aligned}
& \text{maximize} && f_0(x) \\
& \text{subject to} && f_i(x) \leq 0, \quad i = 1, \dots, m \\
& && a_i^T x = b_i, \quad i = 1, \dots, p
\end{aligned} \tag{2.44}$$

as a convex optimization problem if the cost function f_0 is concave, and the inequality constraint functions f_1, \dots, f_m are convex. It is a maximization problem which is readily solved by minimizing the convex cost function $-f_0$ in Section 2.3.

2.3.3 Karush-Kuhn-Tucker optimality conditions

In mathematics, the KKT conditions (also known as Kuhn-Tucker conditions) are necessary for a solution in nonlinear programming to be optimal, provided that some regularity conditions are satisfied. Allowing inequality constraints, the KKT approach to nonlinear programming generalizes the method of Lagrange multipliers, which allows only equality constraints.

Let us consider a nonlinear optimization problem where we want to minimize function $L(x)$, with given constraint,

$$\begin{aligned}
& \text{minimize} && L(x) \\
& \text{subject to} && f(x) \leq 0,
\end{aligned}$$

and x_0 is the optimal value to be found. In that case, the constraint is active if

$$\left. \frac{\partial L}{\partial x} \right|_{x_0} = 0, \tag{2.45}$$

or the constraint is inactive for all admissible values of x when

$$\left. \frac{\partial L}{\partial x} \right|_{x \in S} = 0, \quad (2.46)$$

where S is the set of all admissible values of x . Therefore,

$$\frac{\partial L}{\partial x} + \frac{\partial f}{\partial x} = 0, \quad \text{for } \lambda \geq 0. \quad (2.47)$$

We can write the Lagrangian as

$$\mathcal{L}(x, \lambda) = L(x) + \lambda f(x), \quad (2.48)$$

where the necessary conditions are

$$\frac{\partial \mathcal{L}}{\partial x} = 0 \quad (2.49)$$

$$f(x) \geq 0, \quad (2.50)$$

and

$$\lambda \geq 0, \text{ if } f(x) = 0, \quad (2.51)$$

$$\lambda = 0, \text{ if } f(x) < 0. \quad (2.52)$$

When there are no inequality constraints, the KKT conditions turn into the Lagrange conditions, and the KKT multipliers are called Lagrange multipliers.

3. FREQUENCY MULTIPLEXING AND SINGLE CARRIER FDMA

This chapter provides an introduction of frequency multiplexing that contains both OFDM and single carrier modulation with frequency domain equalization and also provides a brief introduction of single carrier frequency division multiple access systems, subcarrier mapping of SC-FDMA and comparison of both OFDMA and SC-FDMA.

3.1 Frequency Multiplexing

3.1.1 Orthogonal frequency division multiplexing

Orthogonal frequency division multiplexing is a multicarrier transmission technique, which divides the available frequency spectrum into many subcarriers, each one modulated by a low rate data stream. OFDM is similar to the traditional frequency division multiple Access (FDMA) in which the multiple user access is achieved by dividing the available bandwidth into subbands that are allocated to users and requires guard bands between the adjacent subcarriers. However, OFDM uses the available frequency spectrum much more efficiently by spacing the channels much closer together with acquisition of using orthogonal subcarriers to each other. In other words, the orthogonal subcarriers overlap in the frequency domain by preventing interference between the closely spaced subcarriers. OFDM multiplexes the data that will be transmitted on multiple subcarriers and transmits them in parallel as shown in Figure 3.1 [31].

Minimum frequency spacing, Δf is placed between the each orthogonal subcarrier. No subcarrier has power on the center frequencies of the other subcarriers. The spectrum of one orthogonal signal has a

$$\text{sinc}(x) = \sin(x)/x \quad (3.1)$$

shape and each of them is constant over one symbol period T .

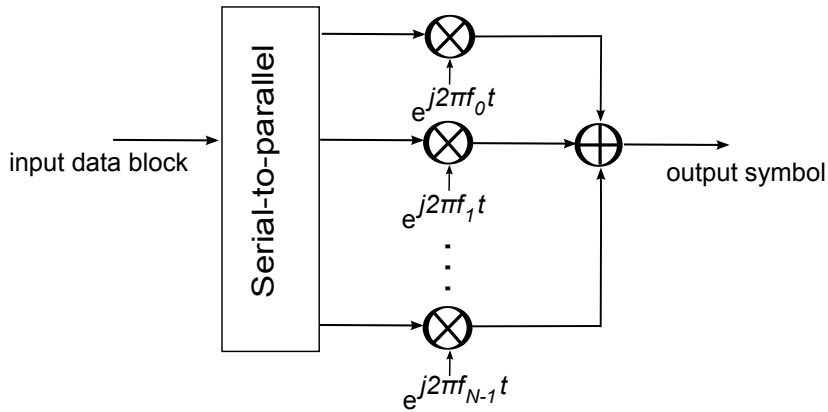


Figure 3.1: A general multi-carrier modulation system [31].

3.1.1.1 OFDM: signal processing

OFDM divides a high-speed digital signal into several slower signals and transmit each slower signal in a separate frequency band. The main idea of OFDM is to eliminate ISI of radio channel that is caused by delay spread of the channel. The slower the signal or in other words, frequency band, the symbol duration is longer. Thus, the symbol is long enough to essentially eliminate ISI. Besides, even the radio channel changes very fast that is called frequency selective or fast fading as described in Section 2.1.3.2.

In order to eliminate intersymbol-interference, frequency division usage was first applied in military communication system, Kineplex, in the 1950s using analog radio technology. The use of orthogonal signals to carry the different low-speed signals was introduced in 1960s, and the roots of current technology based on digital signal processing was introduced in early 1970s [31].

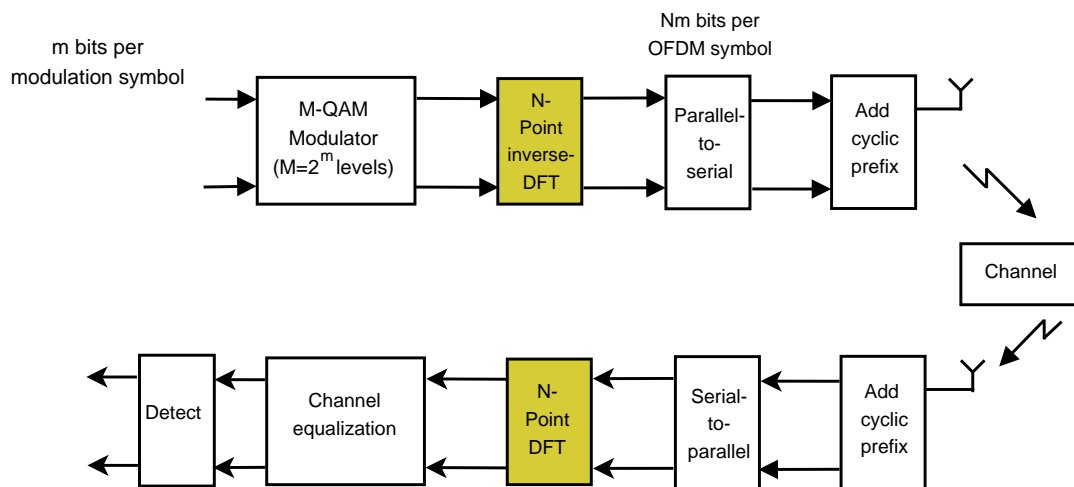


Figure 3.2: Essential OFDM signal processing.

Figure 3.2 shows the essential block diagram of transmitter and receiver of an OFDM using digital signal processing technology. The DFT and IDFT are the fundamental digital signal processing components of OFDM implementation. Realization of DFT and IDFT are much time consuming in real life, so instead of using DFT and IDFT, fast Fourier transform (FFT) and its inverse (IFFT) are used, respectively. Four block of the transmitter of OFDM system can be assumed OFDM modulator. The binary input of the OFDM modulator is the output of of a channel/error coder that introduces error coding code that eliminates channel error caused by noise and fading and also introduces cyclic redundancy check to the information signal to be transmitted. The baseband modulator is generally performing quadrature amplitude modulation (QAM). It converts the binary input signal into a sequence of complex valued multilevel modulation symbols.

After the modulator part, the IDFT performs to produce one OFDM symbol that consisting of one transformed modulation symbol in each of N frequency sub-bands that has m bits per modulation symbol. The IDFT creates the N sub-band samples that are sequentially transmitted through a fading channel. At the receiver part, a DFT performs to recover the N time-domain modulation symbols from the received frequency domain representation. Linear distortion that introduced by multipath propagation of fading channel is compensated by the channel equalization part at the receiver. Finally, a detector produces binary outputs with respect to constellation map that is defined in the OFDM transmitter.

Small scale fading based on channel frequency dependence is explained in Section 2.1.3.2. A signal is affected by frequency-selectivity of a wireless channel if maximum rms delay spread of the channel τ_{max} is larger than the symbol period of the transmitted signal T_s ($\tau_{max} > T_s$), the wireless channel becomes a channel frequency-selective fading; so the channel is affected by ISI. The basic concept of OFDM is to eliminate ISI. Therefore, the symbol period of each subcarrier should be greater than the maximum rms delay spread of the channel, ($T_{sub} > \tau_{max}$). The subcarrier symbol period is directly proportional to the number of subcarriers : $T_{sub} = N * T_{mod}$, where T_{mod} seconds is the duration of a modulation symbol. Therefore, the minimum number

of subcarriers N is determined by:

$$N > \frac{\tau_{max}}{T_{S_{mod}}}. \quad (3.2)$$

Assume that a channel with maximum rms delay spread of $20\mu s$ and a transmission technique with modulation symbol of duration $0.13\mu s$, then $N > 153$ subcarriers. It is always assumed that the number of subcarriers is power of 2, so the number of subcarriers must be 256. Specifically, LTE uses 512 subcarriers in 5 MHz channels.

The aim of the previous operation is to eliminate ISI from the slow signals in the different subcarriers; but the maximum delay spread of the channel can still cause interference between the successive OFDM symbols. In order to eliminate this kind of inter-symbol interference, OFDM system add a guard time, τ_g seconds, between the successive OFDM symbols [31]. The duration of guard time has to be longer than the maximum rms delay spread of the channel, $\tau_g > \tau_{max}$. This guard time contains G modulation samples, during the guard time, at the beginning of each OFDM symbol transmission interval, the transmitter reproduces and transmit the final G transformed modulation signals that generated by the IDFT processor. The G modulation samples transmitted during the guard time is known as the cyclic prefix (CP) of the OFDM symbol. Figure 3.3 illustrates the basic concept of adding cyclic prefix.

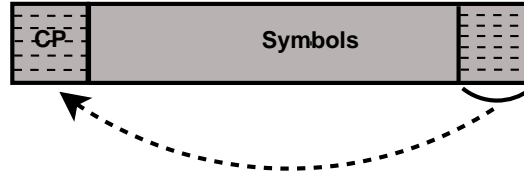


Figure 3.3: Cyclic prefix.

In addition, frequency domain multiplication is equivalent to time domain circular convolution in DFT process. Without CP, the convolution at the receiver is linear convolution and it has to be converted into circular convolution. Frequency domain multiplication becomes circular convolution by adding cyclic prefix at the beginning of the OFDM symbol.

3.1.2 Single carrier modulation with frequency domain equalization

An equalizer compensates for linear distortion that is caused by multipath propagation of the wireless radio channel. Conventional time domain equalizers are complex but

competence for the traditional single carrier transmission system. On the other hand, conventional time domain equalizers are impractical because of the very long channel impulse response in the time domain for broadband channels.

Channel equalization can be explained as inverse filtering of the linear distortion caused by multipath propagation. If a system is linear time invariant, then, linear filtering is a convolution operation in the time domain and a point-wise simple multiplication operation in the frequency domain.

Figure 3.4 shows the basic operation of time domain equalization that is convolution of output signal y and inverse of channel impulse response h^{-1} and frequency domain equalization that is point-wise multiplication of Fourier transform of output signal Y and Fourier transform of inverse of channel impulse response. Basically, the Fourier transform of input signal X can be found by dividing the Fourier transform of output signal point-to-point by an estimate of the channel frequency response. The frequency

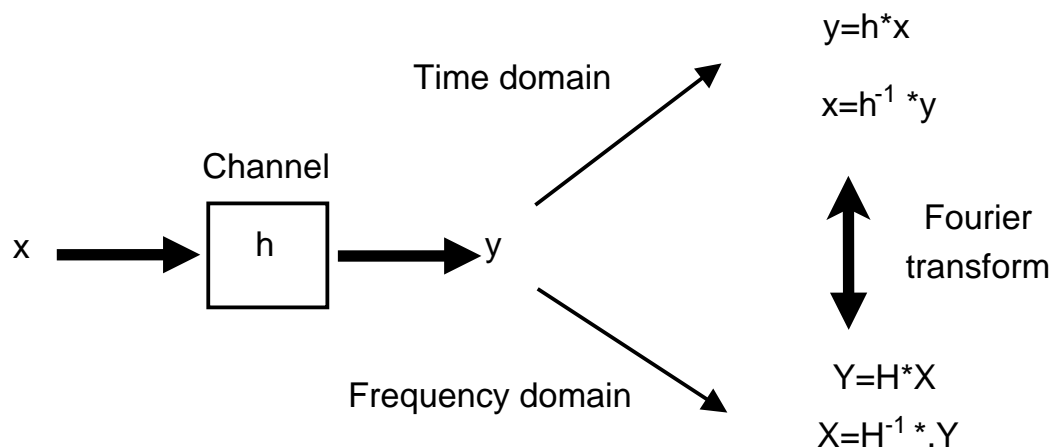


Figure 3.4: Basic idea behind FDE.

domain equalization can be easily implemented with digital signal processors because it doesn't require convolution. The complexity of the FDE is much lower than the equivalent time domain equalizer for broadband channels.

Single carrier FDE has almost the same performance as OFDM with essentially the same overall complexity, even if for a long channel impulse response exists [31]. Figure 3.5 shows the block diagram of both OFDM receiver and SC/FDE receiver systems. As it is shown in figure that both systems have the same communication blocks and the only difference between them is the location of the IDFT block. Unlike

the IDFT block of OFDM is placed in before the adding CP block of the transmitter, the IDFT block of SC/FDE is placed in after the equalization block of the receiver. It can be considered that both of the systems have almost the same link level performance and spectral efficiency.

In OFDM, modulator transmits modulation symbols with different subcarriers in parallel, simultaneously. On the other hand, in SC/FDE, modulator transmits modulation symbols sequentially over N subcarriers. Visually, the OFDM signal is clearly multicarrier and the SC/FDE signal looks like single carrier, which explains the "SC" in its name.

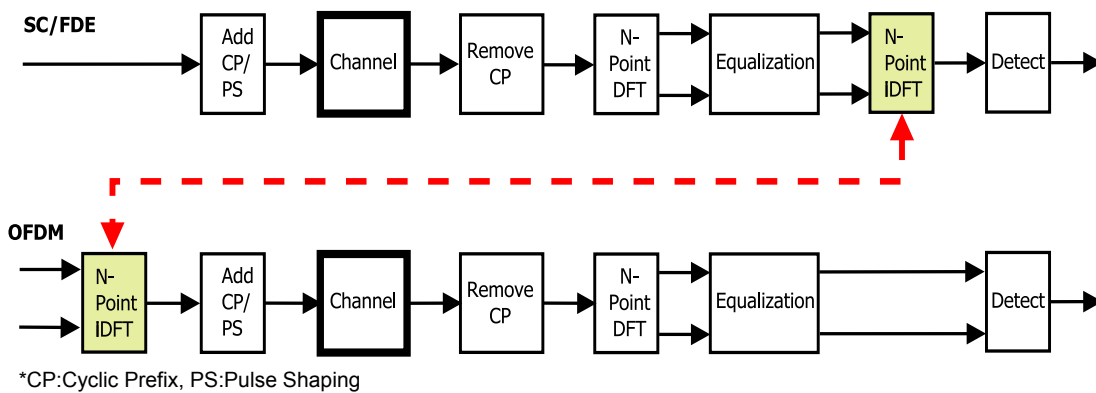


Figure 3.5: Block diagrams of SC/FDE and OFDM systems.

Even though OFDM and SC/FDE are similar in many ways, there are significant differences between them. The main differences are in the nature of equalizer that make the two systems perform differently. Figure 3.6 shows the receivers of both OFDM and SC/FDE. SC/FDE performs both a DFT and IDFT in the receiver, whereas OFDM performs only DFT in the receiver. The IDFT block of OFDM is performed in the transmitter.

SC/FDE receiver transforms the received signal into the frequency domain by applying DFT block, then it performs equalization in the frequency domain. Most of the well-known time domain equalizers, such as MMSE equalizer, decision feedback equalizer and turbo equalizer can be applied for equalization in SC/FDE in the frequency domain. After equalization, an IDFT block transforms the single carrier signal back to the time domain and then a detector estimates the original modulation symbols, whereas OFDM employs a separate equalizer and detector for

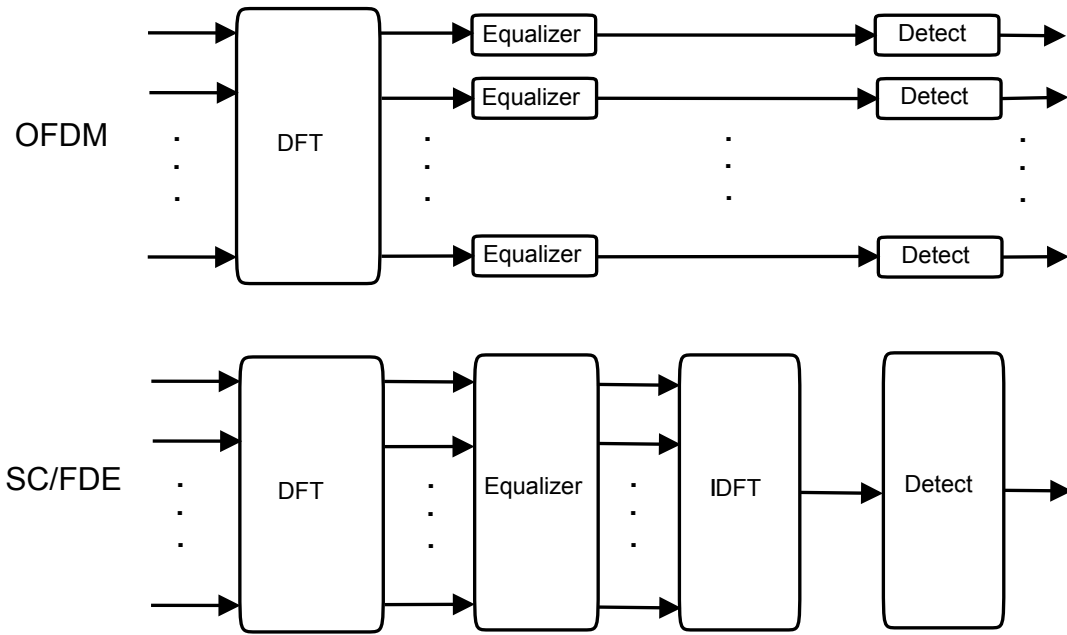


Figure 3.6: OFDM and SC/FDE receivers.

each subcarrier. In other words, SC/FDE performs data detection in time domain after the IDFT block, whereas OFDM performs in the frequency domain. As a result of this, OFDM is more sensitive to a null in the channel spectrum and in order to overcome this sensitivity, it requires channel coding or power/rate control [31].

3.1.3 Comparison of OFDM and SC/FDE

A multipath channel causes inter-symbol interference in the time domain and frequency selectivity in the frequency domain. There are two practical solutions to overcome the effects of a multipath channel ,OFDM and SC/FDE. Both of the systems are explained in previous sections in detailed. In summary, similarities and dissimilarities of the both systems are tabulated in Table 3.1.

3.2 Single Carrier FDMA

OFDMA and SC-FDMA are multiple access methods of OFDM and SC/FDE schemes described in section 3.1.1 and section 3.1.2, respectively. Section 3.1 presents frequency domain multiplexing for only one signal, however, the multiple access techniques that will be presented in this section transmit several signals simultaneously. Due to the natural structure of all the orthogonal frequency division techniques

Table 3.1: Comparison between OFDM and SC/FDE [31].

| | OFDM | SC/FDE |
|-----------------|---|--|
| Similarities | <ul style="list-style-type: none"> *The same performance and structure *DFT/IDFT-based implementation and use of cyclic prefix *Frequency domain equalization *Lower complexity than conventional time domain equalizer | |
| Dissimilarities | <ul style="list-style-type: none"> *Multi-carrier transmission *Parallel transmission of the data with low individual symbol rate *High peak-to-average power ratio *Sensitive to spectral null *Frequency-selective adaptive bit/power loading possible | <ul style="list-style-type: none"> *Single carrier transmission *Sequential transmission of the data with high individual symbol rate *Low peak-to-average power ratio *Less sensitive to frequency offset *Frequency-selective adaptive bit/power loading not possible |

assign a discrete set of orthogonal subcarriers that are distributed across the entire bandwidth. Both of OFDM and SC/FDE perform discrete transforms to move signals between the time domain and frequency domain. In order to transmit several signals simultaneously, multiple access methods assign the signals to predefined exclusive sets of subcarriers, particularly the set of subcarriers is called chunk for SC-FDMA.

As described in Section 2.1.3.2, broadband channels experience frequency-selective fading. The FDMA techniques can employ channel dependent scheduling to achieve multi-user diversity. In addition, the channel characteristics of the user in different locations are statistically independent, so the scheduling techniques can assign each user to subcarriers with favorable transmission characteristics at the location of the user [31].

The Worldwide Interoperability for Microwave Access (WiMAX) cellular system uses OFDMA for transmission of signals both uplink transmission, that is from mobile terminals to base stations, and downlink transmission, that is from base stations to mobile stations. In contrast, due to the 3GPP, LTE uses OFDMA for downlink transmission and SC-FDMA for uplink transmission in order to make the mobile terminal power-efficient.

The major disadvantage of OFDMA is the high peak-to-average power ratio. High PAPR raises the cost because of requirement of the wide linear amplification region of a power amplifier and lowers the power efficiency of the power amplifier. SC-FDMA transmission technique provides lower PAPR due to OFDMA transmission technique considerably. With a lower PAPR, the power amplifiers at mobile terminals employing SC-FDMA can be simpler and more power efficient than they would be with OFDMA transmission. On the other hand, there is a tradeoff between power efficiency and complexity the of frequency domain equalizer of an SC-FDMA system. Since with high signaling rate of SC-FDMA system, the frequency domain equalizer of it is more complicated than a traditional OFDMA equalizer.

3.2.1 SC-FDMA: block diagram

SC-FDMA is a new multiple access technique that utilizes single carrier modulation, DFT spread orthogonal frequency multiplexing, and frequency domain equalization. It has a similar structure and performance as OFDMA. SC-FDMA is currently adopted as the uplink multiple access scheme for 3GPP LTE. Transmitter and receiver structure for SC-FDMA and OFDM are given in Figure 3.7. It is obviously clear from the figure that SC-FDMA transceiver has similar structure as a typical OFDMA system except a new DFT block before subcarrier mapping in transmitter and IDFT block after subcarrier de-mapping in the receiver. Hence, SC-FDMA can be considered as an OFDM system with a DFT mapper.

A transmitter includes a serial to parallel converter, subcarrier mapping, inverse Fourier transform, cyclic prefix addition, parallel-serial conversion, and a digital-to-analog converter followed by an RF modulator. SC-FDMA transmits a block of data symbols simultaneously over one SC-FDMA symbol unlike other modulation techniques that operate symbol by symbol. A SC-FDMA symbol is the time used to transmit all of subcarriers that are modulated by the block of input data symbols.

Actually there is a baseband modulator in front of the serial to parallel converter. The baseband modulator transforms the input binary bits into a set of multi-level complex numbers that corresponds to different modulations formats such as QPSK, QAM. After mapping data bits into modulation symbols, the serial to parallel converter groups

the modulation symbols into a block of N symbols. An N -point DFT transforms these symbols in time domain into frequency domain. Then subcarrier mapping is done in frequency domain. Each frequency domain samples mapped to a subset of M subcarriers where M is greater than N .

To transform the modulated subcarriers in frequency domain to time domain samples an IFFT is used.

The basic idea of cyclic prefix is to replicate part of the SC-FDMA time-domain waveform from the back to the front to create a guard period. As a guard interval, it eliminates the ISI from the previous symbol. Also CP convert linear convolution to circular. The length of the cyclic prefix depends on the channel delay spread, and is preferably longer than the length of the channel response. At the receiver, the prefix part of the symbol is thrown away as it may contain ISI from its previous symbol. Hence, it removes the effect of ISI caused by the multipath signal propagation. However, the prefix is the overhead in an SC-FDMA system, as it does not carry any useful information. The block of complex samples are then serialized in the time domain and converted to analog signals. The RF section modulates the I-Q samples to final transmission radio frequency.

A corresponding receiver does the inverse operations of the transmitter in the reverse order. A typical SC-FDMA receiver includes an RF section, analog-to-digital converter (ADC), parallel-to-serial converter, cyclic prefix remover, Fourier transformer, sub-carrier de-mapper, equalizer, inverse Fourier transformer and detector.

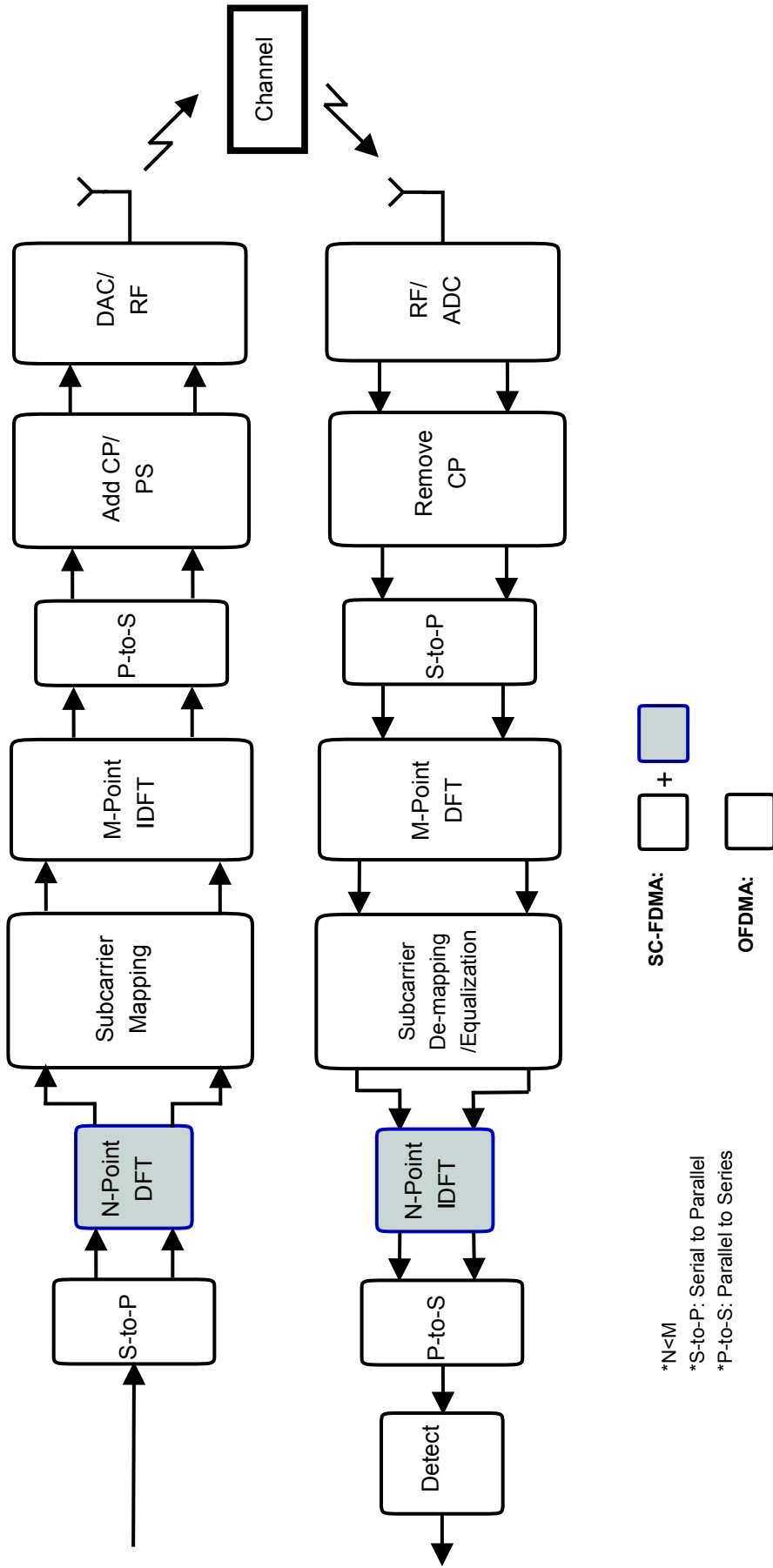


Figure 3.7: Transmitter and receiver structure of SC-FDMA and OFDMA systems.

3.2.2 SC-FDMA: signal processing

Figure 3.7 illustrates how one block of data of SC-FDMA transmitter is sent. The input of the transmitter and the output of the receiver are complex I-Q modulation symbols. Nowadays, adaptive modulation techniques are used depending on the instant channel state, using binary phase shift keying (BPSK) in weak channels and up to 64-level quadrature amplitude modulation (64-QAM) in strong channels. The input data block of transmitter consists of M complex modulation symbols generated at a rate R_{source} symbols/second.

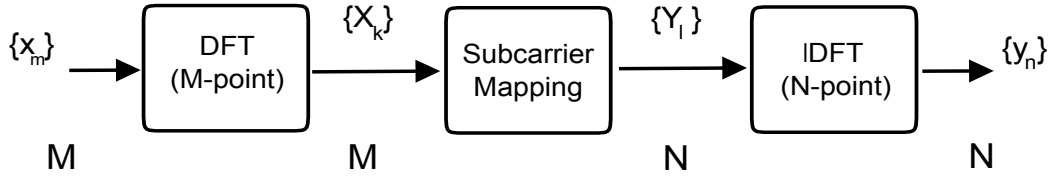


Figure 3.8: Generation of SC-FDMA transmit symbol; there are N subcarriers among which $M(< N)$ subcarriers are occupied by the input data.

Figure 3.8 shows three center elements of the transmitter in detailed. The M -point DFT produces M frequency domain symbols that modulate M out of N orthogonal subcarriers spread over a bandwidth

$$W_{channel} = N \cdot f_0 \quad [Hz] \quad (3.3)$$

where f_0 Hz is the subcarrier spacing. The channel transmission rate is

$$R_{channel} = \frac{N}{M} \cdot R_{source} \quad [symbols/second]. \quad (3.4)$$

If Q denotes the bandwidth spreading factor, i.e.,

$$Q = \frac{R_{channel}}{R_{source}} = \frac{N}{M} \quad (3.5)$$

then, the SC-FDMA system can handle up to to Q orthogonal source signals with each source occupying a different set of M orthogonal subcarriers.

In the notation of Figure 3.8, $x_m(m = 0, 1, \dots, M - 1)$ represents modulated source symbols and $X_k(k = 0, 1, \dots, M - 1)$ represents M samples of the DFT of x_m . $Y_l(l =$

$0, 1, \dots, N - 1$) represents the frequency domain samples after subcarrier mapping and $y_n(n = 0, 1, \dots, N - 1)$ represents the transmitted time domain channel symbols obtained from the inverse DFT of Y_l . The subcarrier mapping block assigns frequency domain modulation symbols to subcarriers. This process is also called as *scheduling*. Since spatially dispersed terminals have independently fading channels, SC-FDMA and OFDMA can benefit from channel dependent scheduling due to the channel characteristics. The inverse DFT that is N -point, ($M < N$), in Figure 3.8 produces a time domain representation, y_n of the N subcarrier symbols. The parallel-to-serial convertor orders y_0, y_1, \dots, y_{N-1} in a time sequence for modulating a radio frequency carrier and transmitter to the receiver [31].

As described detailed in Section 3.1.1.1, it is required to insert a set of symbols referred to as CP in order to prevent inter-block-interference (IBI) due to the multipath propagation. The transmitter also performs a linear filtering operation called as pulse shaping in order to reduce out-of-band signal energy after the parallel-to-serial operation. One of the commonly used pulse shaping filter is a raised-cosined filter. The frequency domain and time domain representations of the filter are as follows:

$$P(f) = \begin{cases} T & , 0 \leq |f| \leq \frac{1-\alpha}{2T}, \\ \frac{T}{2} \{1 + \cos [\frac{\pi T}{\alpha} (|f| - \frac{1-\alpha}{2T})]\} & , \frac{1-\alpha}{2T} \leq |f| \leq \frac{1+\alpha}{2T}, \\ 0 & , |f| \geq \frac{1+\alpha}{2T}, \end{cases} \quad (3.6)$$

$$p(t) = \frac{\sin(\pi t/T)}{\pi t/T} \cdot \frac{\cos(\pi t/T)}{1 - 4\alpha^2 t^2/T^2} \quad (3.7)$$

where T is the symbol period and α is the roll-off factor.

Figure 3.9 illustrates the raised-cosine filter for both frequency domain and time domain for various roll-off factor, α , values. The roll-off factor α ranges from 0 to 1 and controls the amount of out-of-band radiation. With $\alpha = 0$, the filter is an ideal bandpass filter that suppresses all out-of-band radiation as can be shown frequency spectrum of the raised-cosine filter. When α increases from 0 to 1, the out-of-band radiation increases too. From the point of view of the time domain, the side lobes of the impulse response of the raised-cosine filter increases as α decreases. As a result of this, the peak power of the transmitted signal is increased after pulse shaping operation.

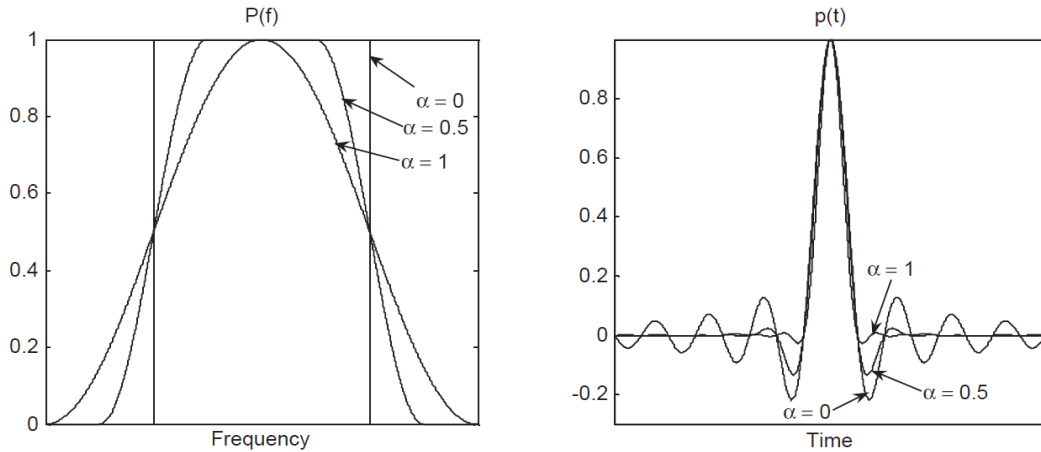


Figure 3.9: Raised-cosine filter [31].

Therefore, with combining these two issues, the choice of the roll-off factor requires a trade-off between the goals of low out-of-band radiation and low peak-to-average power ratio [31].

In order to recover N subcarriers in the receiver, the DFT operator in the receiver as shown in Figure 3.7 transforms the received signal from the time domain to the frequency domain. After DFT operation, the de-mapping operation isolates the M frequency domain samples of each source signal obtained from DFT operator. As referred from the name of SC-FDMA uses single carrier modulation, it is sustained from substantial linear distortion manifested as ISI. The IDFT of the receiver in Figure 3.7 transforms equalized symbols bank into the time domain. Finally, the detector produces the received sequence of M modulated symbols.

From the point of view of multiple user access, SC-FDMA receiver operation is showed in Figure 3.10. The base station separates the users in the frequency domain during the subcarrier de-mapping process in order to perform basic SC-FDMA demodulation process. As shown in Figure 3.10, there are Q users in the system and each of them has individual equalizer process, so demodulation of each user does not affect to the other users. This is one of the biggest difference due to OFDMA.

3.2.3 Comparison with OFDMA

The main difference between OFDMA and SC-FDMA is DFT block at transmitter and IDFT block at receiver. Based on this structure, the reasons for some of its names, such

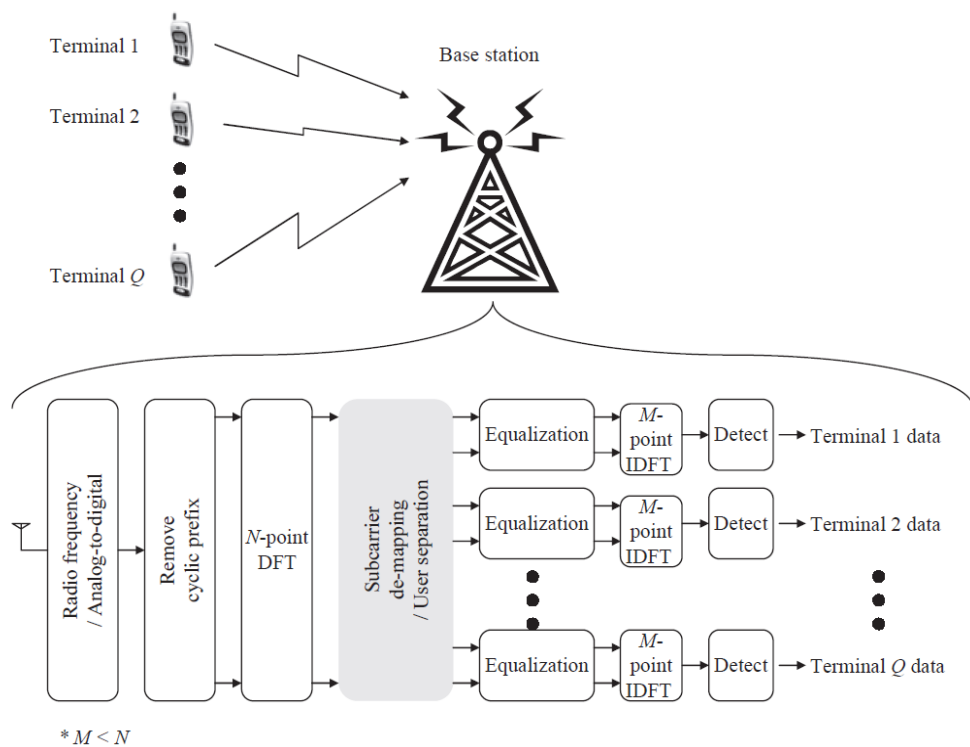


Figure 3.10: SC-FDMA receiver structure from a multiple user access perspective with Q terminals in the uplink [31].

as DFT-pre-coded OFDM or DFT-spread OFDM, are clear. But for the use of "single carrier" in its name, SCFDMA, is not as obvious and is often the reason why is not explained. Unlike the standard OFDM where the each data symbol is carried by the individual subcarriers, the SC-FDMA transmitter carries data symbols over a group of subcarriers transmitted simultaneously. In other words, the group of subcarriers that carry each data symbol can be viewed as one frequency band carrying data sequentially in a standard FDMA.

In Figure 3.11 transmit sequence of and 8 QPSK modulated symbol signal in both OFDMA and SC-FDMA is shown where only 4 subcarriers exist. It is understand from the figure that in OFDMA, each symbol ia transmitted with different subcarriers in parallel while in SC-FDMA each symbol is transmitted by N subcarriers where N is the block length of DFT. Visually, the OFDMA signal is clearly multi-carrier and the SC-FDMA signal looks more like single-carrier, which explains the "SC" in its name.

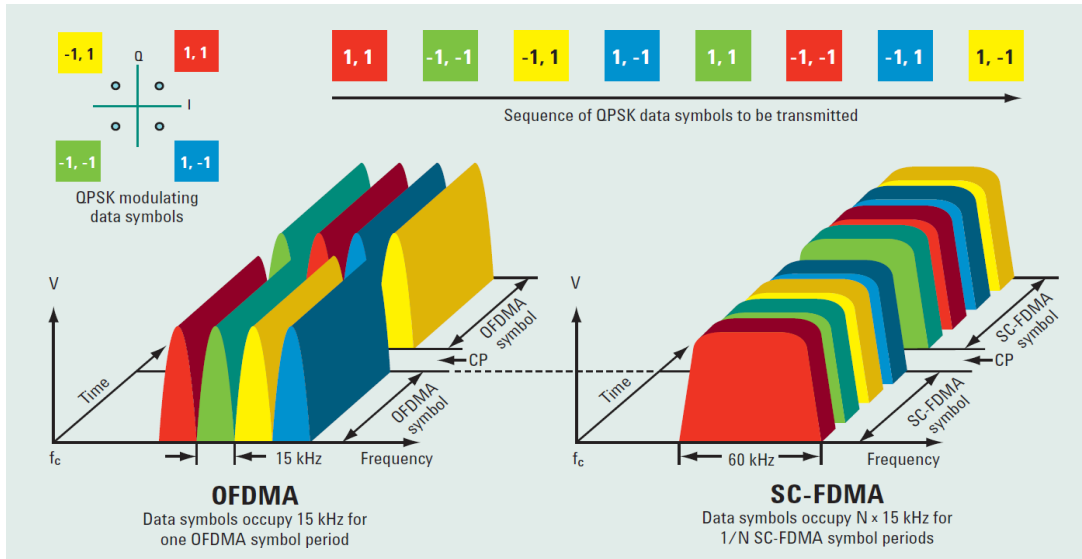


Figure 3.11: Comparison of SC-FDMA and OFDMA transmit sequence of QPSK symbols [32].

Similarities of OFDMA and SC-FDMA is block-based data modulation and processing, division of the transmission bandwidth into narrower sub-bands, frequency domain channel equalization process, and the use of CP.

3.2.4 Subcarrier mapping

In multicarrier systems, the broadband channel is divided into subcarriers which are narrower and orthogonal to each other as mentioned before. The system has more than one user and more than one subcarrier. So the subcarriers have to be assigned to the users in a properly and efficiently way.

In SC-FDMA systems, there are two ways to map subcarriers to the user that are *localized* and *distributed* subcarrier mapping. In addition to this, if there is equidistant between the subcarriers in distributed subcarrier mapping, it is called *interleaved* subcarrier mapping. The subcarriers are adjacent to each other in localized subcarrier mapping and interleaved along to frequency in distributed subcarrier mapping.

Figure 3.12 shows the two arrangements in the frequency domain. There are three terminals, each of them transmitting symbols on four subcarriers in a system with total of 12 subcarriers. In the distributed arrangement, terminal 1 uses subcarriers 0, 3, 6, 9; in the localized arrangement, terminal 1 uses subcarriers 0, 1, 2, 3. After assigning

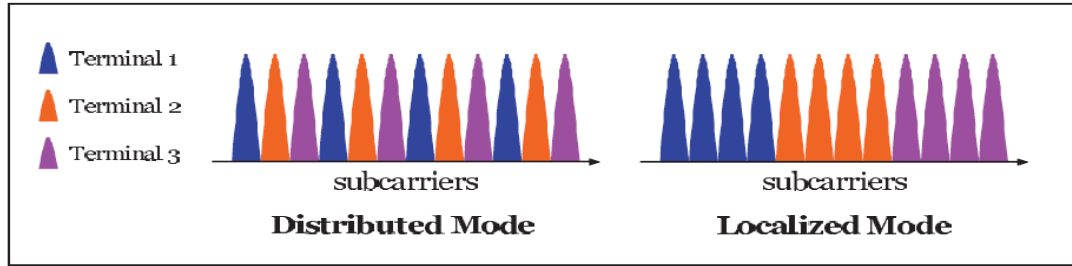


Figure 3.12: Types of SC-FDMA subcarrier mapping [2].

subcarriers to the users, rest of the subcarriers that aren't used have to be assigned as zero.

Distributed SC-FDMA is robust against frequency selective fading because its information is spread across the entire signal band. Therefore, it offers the advantage of frequency diversity. On the other hand, localized SC-FDMA can potentially achieve multi-user diversity in the presence of frequency selective fading [2].

3.2.5 Peak-to-average-power ratio of SC-FDMA

OFDMA is a breakthrough in communication systems. It destroys the frequency selective fading using narrower subbands. Although high performance of OFDMA, it has higher peak to average power ratio which is undesirable for mobile communication systems. High PAPR requires wide linear power amplifier region to transmit signal in the transmitter. For uplink transmission, it is expensive and has higher power consumption because the transmitter is mobile. SC-FDMA is proposed for uplink because of the high peak to average power ratio of the OFDMA.

Although PAPR of SC-FDMA is lower than PAPR of OFDMA system, PAPR is changeable due to the subcarrier mapping type of SC-FDMA.

Figure 3.13 shows an example of SC-FDMA transmitting symbols in the frequency domain for $N=4$ subcarriers per chunk, $Q=3$ users, and $M=12$ subcarriers in the system $X_{l,distributed}$ denotes transmit symbols for interleaved subcarrier mapping and $X_{l,localized}$ denotes transmit symbols for localized subcarrier mapping.

x_n sequence represent time domain symbols. X_k sequence is the DFT coefficients of the x_n sequence. As mentioned in Section 3.2.4, subcarrier mapping is done in frequency domain in SC-FDMA systems. In Figure 3.13, both distributed and localized subcarrier

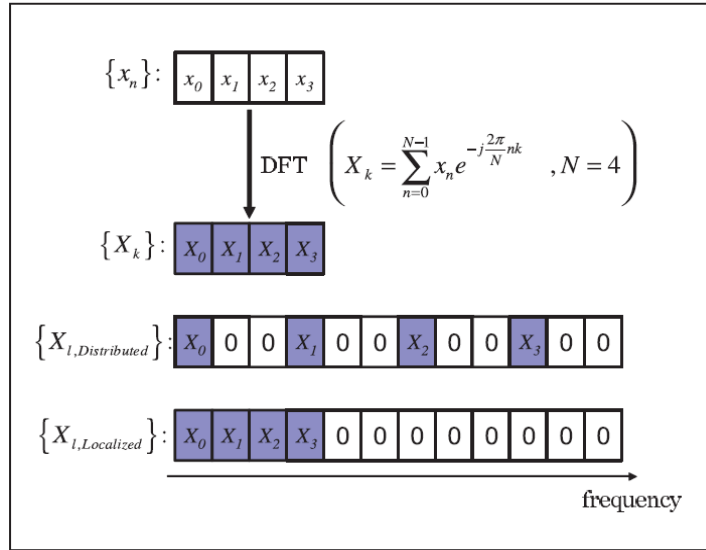


Figure 3.13: An example of SC-FDMA symbol in frequency domain [2].

mapping are shown, respectively. Unused subcarriers are assigned as zero in both cases. In order to obtain subcarriers M-point IDFT has to be applied to symbols.

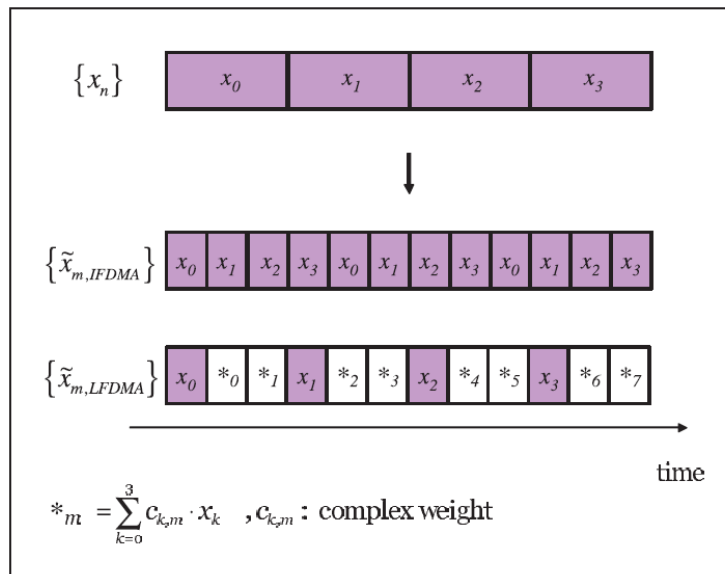


Figure 3.14: An example of SC-FDMA transmit symbols in the time domain [2].

Figure 3.14 shows an example of SC-FDMA transmitting symbols in time domain for $N=4$ subcarriers per chunk, $Q=3$ users, $M=12$ subcarriers. After taking M -point IDFT of X_k at the receiver part, symbols are transmitted in time domain. As mentioned in Section 3.2.4, subcarrier mapping can be scheduled either localized or distributed (interleaved) arrangement, so transmission in time domain differs for both of these arrangements. If the subcarrier mapping is scheduled as interleaved mode, data

symbols are conveyed in time domain consecutively. But if the subcarrier mapping is scheduled as localized mode, randomly generated complex weights (ck, m) appear between the data symbols. Because of these randomly generated complex weights in localized mapping, fluctuations occur in time domain, so the peak value of the symbols is bigger than the average value of the symbols or PAPR is bigger than 1 called. In contrast, if all the symbols have same energy to be transmitted, PAPR doesn't occur in the interleaved mapping because randomly generated complex weights doesn't seen in interleaved mode. But if all the symbols don't have the same energy (16-QAM, 32-QAM ,etc.), PAPR occurs in this mapping too but not as much as in localized mode but PAPR of both localized and interleaved mapping is not as much bigger as PAPR of OFDMA. Additional disadvantages of OFDMA compared to SC-FDMA are the strong sensitivity to carrier frequency offset and strong sensitivity to nonlinear distortion in the power amplifier due to the high PAPR [2].

4. SUM-RATE OPTIMAL RESOURCE ALLOCATION

4.1 Introduction

This chapter presents one of the main advantage of single carrier frequency division multiplexing access - the opportunity to apply channel dependent scheduling in the process of subcarrier mapping for both localized and interleaved schemes and thereby obtain performance improvements due to multi-user diversity. In radio environment, radio channels with wide bandwidth may experience frequency selective fading. The consequence of this frequency selective nature of broadband channel transfer functions is channel dependent scheduling of pair of subcarriers and users. When users are dispersed spatially, each one has a different channel transfer function. Subcarrier assignment for different users have to be scheduled due to the channel conditions to increase total system throughput.

Figure 4.1 shows the frequency responses of channels assigned two different users and is represented as the square root of the channel gain at each of 256 subcarriers. If the access system has these two users and 256 subcarriers, how can these subcarriers be allocated to the users? The channel dependent scheduling can solve this problem in a optimal way. In addition to this, a practical system would have to monitor periodically the channel impulse responses of the users who is sharing the broadband frequency band and devise a new schedule matched to the current frequency responses of all the users.

For a SC-FDMA system, the jointly optimal power and chunk allocation policies which maximize the sum rate are obtained in this thesis. The proposed solution is applicable to both localized and interleaved subcarrier mapping schemes. The joint optimization problem is solved by sequentially solving two sub-problems: power allocation and chunk allocation. Primarily, an optimal power allocation algorithm is used, which is derived from Karush-Kuhn-Tucker conditions; and then the optimum chunk assignment problem is converted into a maximum weighted matching problem

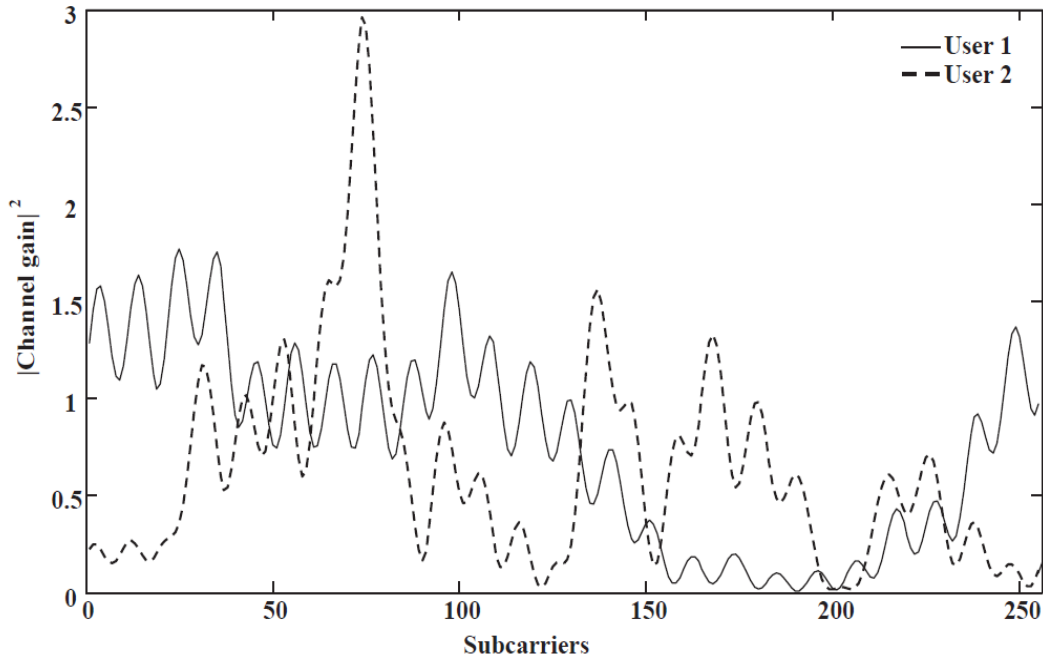


Figure 4.1: Channel impulse response of two different user [31].

on a bipartite graph, and hence is solved in polynomial time. Two greedy chunk allocation algorithms with lower complexity are also proposed, and demonstrated that these algorithms produce near optimal results, especially for interleaved subcarrier mapping, when used in conjunction with optimal power control.

4.2 System Model

Let consider an SC-FDMA system with B Hz total bandwidth and K users. The total frequency band is divided into L subcarriers of equal bandwidth, B/L . The L subcarriers have to be grouped into several chunks to be allocated to different users. Assuming that the system has N chunks, each of the chunks have $M = L/N$ subcarriers and occupy a bandwidth of B/N Hz. Let also assume that the system is overloaded, i.e., the number of users with data available for transmission is always greater than or equal to the number of chunks. Moreover, in order to maximize the user capacity and preserve fairness, it is assumed that each user can only take one chunk in the system. There are two types of subcarrier mapping methods in SC-FDMA as described in Section 3.2.4: localized FDMA (LFDMA) and interleaved FDMA (IFDMA). In LFDMA, the subcarriers of a chunk are adjacent to each other. In IFDMA, the

subcarriers of a chunk are distributed equidistantly over the entire frequency band in order to avoid allocating adjacent subcarriers in deep fading. In this thesis, both subcarrier mapping approaches are addressed.

The chunk assignment decisions are made at the base station. Thus, let assume that the base station has perfect channel state information (CSI) about the links from the users. Let $h_{i,k}$ denote the channel coefficient of user k on subcarrier i , $p_{i,k}$ denote the power assigned by user k to subcarrier i and $\sigma_{i,k}^2$ is the noise power on subcarrier i for user k . The signal-to-noise ratio (SNR) value for user k on subcarrier i is:

$$\gamma_{i,k} = \frac{p_{i,k}|h_{i,k}|^2}{\sigma_{i,k}^2}. \quad (4.1)$$

Let I_n denote the set of subcarriers called as *chunk*, assigned to each chunk $n \in \{1, \dots, N\}$. Assuming minimum mean square error equalization is performed at the receiver, the rate achievable by each user depends on the equivalent SNR $\gamma_{n,k}$ of user k on chunk n , obtained after MMSE equalization as in [4, 33, 34],

$$\gamma_{n,k} = \left[\frac{1}{\frac{1}{|I_n|} \sum_{i \in I_n} \frac{\gamma_{i,k}}{\gamma_{i,k} + 1}} - 1 \right]^{-1}, \quad (4.2)$$

Plugging (4.1) into (4.2), and after some manipulation, (4.2) becomes

$$\gamma_{n,k} = \left[\left(\frac{1}{|I_n|} \sum_{i \in I_n} \frac{\frac{p_{i,k}|h_{i,k}|^2}{\sigma_{i,k}^2}}{\frac{p_{i,k}|h_{i,k}|^2}{\sigma_{i,k}^2} + 1} \right)^{-1} - 1 \right]^{-1}. \quad (4.3)$$

The main goal is to obtain the optimal power and chunk allocation which jointly maximize the sum rate of the system. Note that, the rate

$$R_{n,k} = (B/N) \log_2(1 + \gamma_{n,k}), \quad (4.4)$$

is achievable by user k , assuming that it transmits on chunk n . Due to the orthogonality of the chunks, the sum rate of the system can simply be computed by adding the rates

achievable on each chunk, i.e.,

$$R_{\text{sum}} = \sum_{n=1}^N \sum_{k=1}^K \omega_{n,k} R_{n,k}, \quad (4.5)$$

$$= \sum_{n=1}^N \sum_{k=1}^K \omega_{n,k} (B/N) \log_2(1 + \gamma_{n,k}), \quad (4.6)$$

where $\omega_{n,k} \in \{0, 1\}$ is an indicator variable, which takes the value 1 if n th chunk is allocated to user k , and 0 otherwise. Since each user is assumed to be assigned at most one chunk, therefore $\sum_n \omega_{n,k} \leq 1$, for all $k \in \{1, \dots, K\}$.

Subcarriers I_n of chunk n can be either consecutive or equidistantly distributed over the entire bandwidth, hence the problem that is solved in this thesis is applicable to both localized and interleaved chunk allocations. In the following section, the problem formulation and the optimality conditions to maximize sum rate of the system is given.

4.3 Joint Power and Chunk Allocation

Plugging (4.3) into (4.6), and after some manipulation, let rewrite the sum rate in terms of the powers $p_{i,k}$:

$$R_{\text{sum}} = - \left(\frac{B}{N} \right) \sum_{n=1}^N \sum_{k=1}^K \left[\omega_{n,k} \log_2 \left(1 - \frac{1}{|I_n|} \sum_{i \in I_n} \frac{p_{i,k} |h_{i,k}|^2}{p_{i,k} |h_{i,k}|^2 + \sigma_{i,k}^2} \right) \right]. \quad (4.7)$$

For simplicity, let us define

$$c_{i,k} = \frac{\sigma_{i,k}^2}{|h_{i,k}|^2}, \quad (4.8)$$

which can be interpreted as the inverse of the normalized channel gain. Then, dropping the constant (B/N) , the problem of maximizing (4.7) is equivalent to

$$\begin{aligned} & \max_{\substack{\omega_{n,k} \\ p_{i,k}}} \sum_{n=1}^N \sum_{k=1}^K \left[- \omega_{n,k} \log_2 \left(1 - \frac{1}{|I_n|} \sum_{i \in I_n} \frac{p_{i,k}}{p_{i,k} + c_{i,k}} \right) \right], \\ & \text{s.t. } \sum_{k=1}^K \omega_{n,k} \leq 1 \quad \forall n, \quad \sum_{n=1}^N \omega_{n,k} \leq 1, \quad \forall k \\ & \quad \sum_{i=1}^M p_{i,k} \leq \bar{P}_k \quad \forall k, \quad p_{i,k} \geq 0, \quad \forall i, k, \end{aligned} \quad (4.9)$$

where \bar{P}_k is the available average power of user k .

Note that, it is rather difficult to jointly optimize the chunks allocated to each user, and powers allocated to each chunk, since the chunk allocation problem itself is a combinatoric problem even without power allocation, and the powers clearly depend on which chunk is selected, through the channel coefficients. Therefore, in what follows, a two step solution is proposed, without compromising optimality:

Proposition 1. The solution to problem derived in (4.9) can be obtained by solving the two step problem

$$\begin{aligned}
& \max_{\omega_{n,k}} \sum_{n=1}^N \omega_{n,k} \sum_{k=1}^K \max_{p_{i,k}} \left[-\log_2 \left(1 - \frac{1}{|I_n|} \sum_{i \in I_n} \frac{p_{i,k}}{p_{i,k} + c_{i,k}} \right) \right], \\
& \text{s.t.} \quad \sum_{k=1}^K \omega_{n,k} \leq 1 \quad \forall n, \quad \sum_{n=1}^N \omega_{n,k} \leq 1, \quad \forall k \\
& \quad \sum_{i=1}^M p_{i,k} \leq \bar{P}_k \quad \forall k, \quad p_{i,k} \geq 0, \quad \forall i, k.
\end{aligned} \tag{4.10}$$

Proof. First, let us fix the chunk allocation coefficients, i.e., $\omega_{n,k}$, to an admissible set that satisfy the conditions in (4.9). The key here is to observe that, fixing $\omega_{n,k}$, $\forall n$ is equivalent to fixing the set of subchannels, say $I_{n,k}$, to be allocated to each user k . But then, the overall sum rate achievable by the users under each fixed chunk assignment can be found by solving

$$\begin{aligned}
& \max_{p_{i,k}} \sum_{k=1}^K \left[-\log_2 \left(1 - \frac{1}{|I_{n,k}|} \sum_{i \in I_{n,k}} \frac{p_{i,k}}{p_{i,k} + c_{i,k}} \right) \right], \\
& \text{s.t.} \quad \sum_{i \in I_{n,k}} p_{i,k} \leq \bar{P}_k \quad \forall k, \quad p_{i,k} \geq 0, \forall i, k.
\end{aligned} \tag{4.11}$$

Due to the orthogonality of the subchannels, the maximization can be carried out separately over each chunk, or equivalently, over each user. Hence, the maximum operation can be moved inside the summation over the users, to yield

$$\begin{aligned}
& \max_{p_{i,k}} \left[-\log_2 \left(1 - \frac{1}{|I_{n,k}|} \sum_{i \in I_{n,k}} \frac{p_{i,k}}{p_{i,k} + c_{i,k}} \right) \right], \\
& \text{s.t.} \quad \sum_{i \in I_{n,k}} p_{i,k} \leq \bar{P}_k \quad \forall k, \quad p_{i,k} \geq 0, \forall i, k.
\end{aligned} \tag{4.12}$$

Let us denote by $R_{n,k}^*$, the maximum achievable rate by each user k over chunk n , obtained from (4.12). Then, (4.9) becomes

$$\begin{aligned} \max_{\omega_{n,k}} \quad & \sum_{n=1}^N \omega_{n,k} \sum_{k=1}^K R_{n,k}^* \\ \text{s.t.} \quad & \sum_{k=1}^K \omega_{n,k} \leq 1 \quad \forall n, \quad \sum_{n=1}^N \omega_{n,k} \leq 1, \quad \forall k \end{aligned} \quad (4.13)$$

which is equivalent to (4.10), since the optimal chunk allocation is in the feasible set, and an exhaustive search over all chunk allocations will clearly yield the global optimum sum rate. \square

In what follows, firstly the inner maximization problem derived in (4.12) will be solved, the optimum power allocation policy for a fixed chunk assignment will be derived, an algorithm to find the optimal power distribution will be proposed. Then, the outer maximization problem in (4.10) will be solved, and efficient optimal and suboptimal algorithms for chunk allocation will be proposed.

4.3.1 Optimal power allocation

Let us start by noting that the cost function in (4.12) is concave, and the constraints form a convex set. Hence, this is a well defined convex optimization problem, with the solution given in the following proposition.

Proposition 2. The optimal power allocation for user k over each subcarrier i is given by

$$p_{i,k} = \left(\sqrt{\frac{c_{i,k}}{\lambda_k}} - c_{i,k} \right)^+, \quad (4.14)$$

where $\lambda_k > 0$ is a real number, selected so that the per user power constraint is satisfied, and $(\cdot)^+$ denotes $\max(\cdot, 0)$.

Proof. Due to the convex nature of the problem, KKT conditions are necessary and sufficient for optimality. Let us define the Lagrangian by

$$\begin{aligned} \mathcal{L} = & -\log_2 \left(1 - \frac{1}{|I_{n,k}|} \sum_{i \in I_{n,k}} \frac{p_{i,k}}{p_{i,k} + c_{i,k}} \right) \\ & + \sum_{k=1}^K \xi_{i,k} p_{i,k} - \mu_k \sum_{k=1}^K (p_{i,k} - \bar{P}_k), \end{aligned} \quad (4.15)$$

where μ_k is the Lagrange multiplier assigned to the power constraint and $\xi_{i,k}$ are the Lagrange multipliers assigned to the non-negativity constraints for the powers. Taking partial derivatives, the KKT conditions,

$$\left(\frac{1}{A}\right) \frac{c_{i,k}}{(p_{i,k} + c_{i,k})^2} - \mu_k + \xi_{i,k} = 0, \quad \forall i, k, \quad (4.16)$$

$$p_{i,k} \xi_{i,k} = 0, \quad \forall i, k, \quad (4.17)$$

$$\sum_{i \in I_{n,k}} p_{i,k} \leq \bar{P}_k, \quad (4.18)$$

are obtained, where,

$$A = \ln 2 \left(1 - \frac{1}{|I_{n,k}|} \sum_{i \in I_{n,k}} \frac{p_{i,k}}{p_{i,k} + c_{i,k}} \right). \quad (4.19)$$

Letting $\mu_k A = \lambda_k$, and combining (4.16) and (4.17), the optimal powers should satisfy

$$\frac{c_{i,k}}{(p_{i,k} + c_{i,k})^2} \leq \lambda_k, \quad (4.20)$$

with equality if and only if $p_{i,k} > 0$ (or else, $\xi_{i,k} > 0$ and strict inequality is get). Solving (4.20) for $p_{i,k}$, and selecting λ_k so that (4.18) are satisfied, the desired result is obtained. \square

The optimal power allocation can be approximately found to within any desired precision using a binary search over the real number λ_k , by selecting an appropriate stopping criterion. In what follows, it is shown that the exact optimal solution may also be found with very low complexity. First, let us prove a useful property of the optimal powers:

Proposition 3. Let $c_{[i],k}$ denote an ordered version of the inverse normalized channel gains $c_{i,k}$, i.e., let $c_{[i],k} < c_{[i+1],k}$, $\forall i, \forall k$. Then, $p_{[i+1],k} > 0$ implies $p_{[i],k} > 0$. Moreover, if $p_{[i+1],k} > 0$, then,

$$p_{[i],k} = \sqrt{\frac{c_{[i],k}}{c_{[i+1],k}} (p_{[i+1],k} + c_{[i+1],k})} - c_{[i],k}, \quad (4.21)$$

Proof. The first part is easily proved by contradiction. Assume $p_{[i+1],k} > 0$ is possible when $p_{[i],k} = 0$. Then, from (4.20) it is needed that

$$\frac{1}{(c_{[i],k})} \leq \lambda_k = \frac{c_{[i+1],k}}{(p_{[i+1],k} + c_{[i+1],k})^2} < \frac{1}{(c_{[i+1],k})}, \quad (4.22)$$

which is a contradiction, as by assumption $c_{[i],k} < c_{[i+1],k}$, thereby proving the first statement. The second statement follows, since $p_{[i+1],k} > 0$ implies $p_{[i],k} > 0$ by the previous statement, and from (4.20), we have

$$\lambda_k = \frac{c_{[i],k}}{(p_{[i],k} + c_{[i],k})^2} = \frac{c_{[i+1],k}}{(p_{[i+1],k} + c_{[i+1],k})^2}. \quad (4.23)$$

Solving for $p_{[i],k}$, and noting that the solution is always positive, so the desired result is gotten. \square

Remark 1. In plain terms, Proposition 3 states that a subcarrier in a chunk can be assigned a non-zero power, only if all subcarriers with stronger channel conditions in the chunk are already used, which is quite intuitive. Note however that, this does not mean the assigned powers have to be monotone increasing in channel gains as in the typical waterfilling solution for OFDMA systems: this interesting observation can be verified by simply considering a 2-subcarrier per chunk scenario and setting $c_{1,k} = 1$, $c_{2,k} = 2$, $\lambda_k = 0.01$ and $\bar{P}_k = 10\sqrt{2} + 7$, which can be shown to satisfy the KKT conditions with powers $p_{1,k} = 9 < 10\sqrt{2} - 2 = p_{2,k}$.

Proposition 3 suggests a natural method for solving the optimization problem exactly without having to search for the real valued λ_k . Let $p_{[i],k} > 0$ for $i = \{1, \dots, m\}$, and $p_{[i],k} = 0$ for $i = \{m+1, \dots, M\}$. It is easy to show that by iterated use of (4.21), all powers can be written in terms of the first non-zero power in the sequence, i.e., $p_{[m],k}$, by

$$p_{[i],k} = \sqrt{\frac{c_{[i],k}}{c_{[m],k}}} (p_{[m],k} + c_{[m],k}) - c_{[i],k}, \quad i = \{1, \dots, m\} \quad (4.24)$$

and substituting this in the power constraint, it is obtained

$$p_{[m],k} = \frac{\bar{P}_k + \sum_{i=1}^m (c_{[i],k} - \sqrt{c_{[i],k}c_{[m],k}})}{\sum_{i=1}^m \sqrt{c_{[i],k}/c_{[m],k}}}. \quad (4.25)$$

Once $p_{[m],k}$ is computed, all other powers can be computed recursively. Note that, one still needs to find the value of m for which $p_{[i],k} > 0$ for $i = \{1, \dots, m\}$ and $p_{[i],k} = 0$ for $i = \{m+1, \dots, M\}$, but since the search space is integers, this can simply be done in at worst M steps (complexity of $\log M$ is also possible by binary search, but a linear search is focused on to keep the algorithm concise), by computing $p_{[m],k}$ using (4.25),

Algorithm 1 Power Allocation

- 1: Fix k, n ; set $m = M$
 - 2: Sort $c_{i,k}$ in ascending order
 - 3: Compute $p_{[m],k}$ using (4.25)
 - 4: **while** $p_{[m],k} \leq 0$ **do**
 - 5: $m=m-1$
 - 6: Compute $p_{[m],k}$ using (4.25)
 - 7: **end while**
 - 8: Compute $p_{[i],k}$ using (4.24)
-

until a positive value is found. The overall algorithm that is used to find optimal powers is summarized as Algorithm 1.

Proposition 4. The complexity of the Algorithm 1 (power allocation algorithm) is $O(M \log M)$.

Proof. In order to find m , there is a while loop in the Algorithm 1. Finding the m value is a binary search. Let us give an example to find complexity of a binary search. Assume sample space is, $M = 1, 3, 4, 6, 8, 9, 11$ and the desired value, $X = 4$.

- Compare X to 6. It is smaller. Repeat with $M = 1, 3, 4$.
- Compare X to 3. It is bigger. Repeat with $M = 4$.
- Compare 4. It is equal. We are done, the desired value found.

This called binary search:the length of the list is halved in each iteration. Therefore, the total number of iterations cannot be greater than $\log M$. In the worst case, the $P_{[m],k} \geq 0$ value can be found in M iterations. Therefore, the complexity of the algorithm is $O(M \log M)$. Since $M = 12$ in a typical SC-FDMA system, the convergence is very fast. □

4.3.2 Optimal and suboptimal chunk allocation

Let us now turn to the problem (4.13), and focus on optimal chunk allocation. Assume that, using Algorithm 1, the optimal power allocation, and hence the maximum achievable rate $R_{n,k}^*$ is computed for all possible user-chunk pairs n, k . The key is to realize that, since each chunk can be assigned to only one user, and vice versa, (4.13)

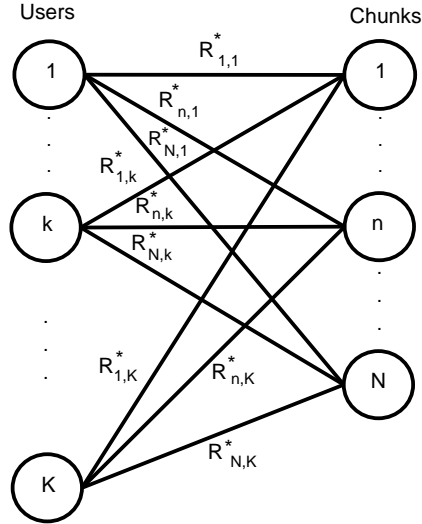


Figure 4.2: Bipartite graph representing matching of users and chunks.

can be stated as a maximum weighted matching problem on a bipartite graph, or in other words an assignment problem, where the weight on the edge connecting each user and chunk is the corresponding power optimized rate, as shown in Figure 4.2. Then, standard techniques from graph theory, such as the Hungarian algorithm, can be used to solve (4.13) in polynomial time and obtain $\omega_{n,k}$ that are jointly optimal with the powers found in Section 4.3.1.

The Hungarian algorithm is a well-known algorithm for maximum weighted matching on a bipartite graph. The computational complexity of the Hungarian algorithm is $O(N^3)$ [35]. The computational complexity of the proposed optimal algorithm is $O(\max(N, K)^3)$. Since the chunk-user matrix is not a square matrix, the maximum of $N - K$ pair has to be found, $\max(N, K)$.

In order to further speed up the chunk assignment problem, two suboptimal greedy algorithms are also proposed in the thesis. The first one, which is called jointly greedy user-chunk allocation, first obtains $R_{n,k}^* \forall k, n$, and then finds the pair $\{\tilde{k}, \tilde{n}\}$ with the highest rate. Next, \tilde{k} and \tilde{n} are deleted from the set of available chunks and users, and the search is repeated until all chunks are allocated.

Proposition 5. The complexity of this algorithm, which is given as Algorithm 2, is $O(N^2K)$, which is less than that of maximum weighted matching, especially with $N < K$.

Proof. The maximum achievable rates $R_{n,k}^* \forall k, n$ obtained by optimal power allocation. A chunk-user matrix, $(N \times K)$, is obtained with these maximum rates. The highest rate of the chunk-user matrix is found in worst case with NK iterations. After finding the highest rate, the row and the column on which the highest rate placed are eliminated. Then, a new chunk-user matrix, $((N - 1) \times (K - 1))$, is obtained with the rest of the rates. The maximum rate of the new matrix is found and the row and the column on which the rate placed are eliminated again. This procedure continues as the number of the chunk, N . Therefore, the computational complexity of the Algorithm 2 is found as $O(N \times (NK)) = O(N^2 K)$. \square

Algorithm 2 Jointly Greedy User-Chunk Allocation

- 1: Compute $R_{n,k}^* \forall k, n$, using Algorithm 1.
 - 2: Initialize $S_U = \{1, \dots, K\}$, $S_C = \{1, \dots, N\}$
 - 3: **for** $j=1:N$ **do**
 - 4: $[\tilde{n}, \tilde{k}] = \arg \max_{n \in S_U, k \in S_C} R_{n,k}^*$
 - 5: Allocate the chunk \tilde{n} to the user \tilde{k}
 - 6: $S_U = S_U - \{\tilde{k}\}$, $S_C = S_C - \{\tilde{n}\}$
 - 7: **end for**
-

The second greedy algorithm that is proposed, which is called greedy user allocation, is a much faster algorithm which simply goes through the chunks only once, and for each chunk, finds the most favorable user among the set of unassigned users, and assigns it to the chunk being considered. The pseudocode of the algorithm is given as Algorithm 3.

The advantage of this algorithm is twofold: it not only runs with much less complexity, but it also can be implemented such that the power optimized rates $R_{n,k}^*$ are computed and ordered on the fly while assigning users to chunks (note that only the maximum for each chunk is needed). Hence, the storage requirement is significantly less, as all user-chunk pairs need not be considered.

Proposition 6. The complexity of this algorithm, which is given as Algorithm 3, is $O(NK)$.

Proof. The chunk-user matrix, $(N \times K)$, is again obtained with the maximum achievable rates. The highest rate is found for the first row (chunk) in worst case with K iterations.

Algorithm 3 Greedy User Allocation

```
1: Initialize  $S_U = \{1, \dots, K\}$ 
2: for  $n=1:N$  do
3:   Initialize  $R_n = 0$ ,
4:   for  $k \in S_U$  do
5:     Compute  $R_{n,k}^*$  using Algorithm 1.
6:     if  $R_{n,k}^* > R_n$  then
7:        $R_n = R_{n,k}^*$ 
8:        $\tilde{k} = k$ 
9:     end if
10:  end for
11:  Allocate user  $\tilde{k}$  to chunk  $n$ 
12:   $S_U = S_U - \{\tilde{k}\}$ 
13: end for
```

The column on which the highest rate of the first row and the first row are eliminated. Then, the highest rate is found for the second row and the column on which the highest rate of the second row is placed and the second row are eliminated. This procedure continues as the number of rows (chunks), N . Therefore, the computational complexity of the Algorithm 3 is found as $O(N \times K) = O(NK)$. \square

In the following chapter, the performance of proposed optimal and suboptimal joint power allocation algorithms are compared.

5. SIMULATIONS AND RESULTS

5.1 Sum-Rate Capacity Simulations

In this thesis, the joint power and chunk allocation problem is solved as described in Chapter 4. Firstly, the problem is divided into two main parts that are power allocation and chunk allocation. Due to the orthogonality of the subchannels, the maximization can be carried out separately over each chunk, or equivalently, over each user. Therefore, it is derived the optimum power allocation policy for a fixed chunk assignment, and proposed an algorithm to find the optimal power distribution, then, proposed efficient optimal and 2 suboptimal algorithms for chunk allocation. All of the proposed 3 algorithms have optimal power allocation for a particular chunk and from the point of view of complexity, 2 suboptimal algorithms are proposed addition to the optimal one. The proposed 3 algorithms, the channel dependent scheduling proposed in [4] and round are compared with each other in the system performance.

Monte Carlo simulation technique is used to demonstrate system total throughput by changing number of users in ascending order. For each user, let us generate Rayleigh channels with each of them arbitrarily has 10ms delay for each user. An additive white Gaussian noise with zero mean is assumed at the receiver. An MMSE equalizer is used and the maximum transmit power of each user is scaled to give a received SNR value of -5dB for each user. Noise power is also assumed as same as for each user. The only difference between the users is that each user has a different channel response from others.

The performance analysis is made for both 16 chunks in the total system with 5 MHz bandwidth and 32 chunks in the total system with 10 MHz bandwidth. It is also assumed that each chunk has $M = 16$ subcarriers and each subcarrier has 19.531 kHz (5 MHz bandwidth/256 subcarriers or 10 MHz bandwidth/512 subcarriers) tone spacing.

In Figures 5.1, 5.2, 5.3, 5.4 and 5.5, the performance of proposed optimal and suboptimal algorithms for joint chunk and power allocation are evaluated by using

Monte Carlo approach, for a system with 16 chunks. In curves labeled LFDMA, chunks with adjacent subcarriers are assigned to users, and in curves labeled IFDMA, equidistantly distributed subcarriers along the entire bandwidth are assigned. The results are compared to [4], which uses equal power for each subcarrier; and two round robin scheduling schemes, labeled R-LFDMA and R-IFDMA. Round robin scheduling means that chunks are randomly assigning to users. Channel dependent scheduling is not taken into account in round robin scheduling, it is independent from channel gains.

Although throughout the thesis assumed that $K > N$, the case with $K \leq N$ was also simulated for completeness, with some necessary modifications to the algorithms. As the number of users is increased, all chunk allocation schemes except for the random round robin scheduling achieve increasing rates, which is due to the diversity created by the additional users. It is evident that localized subcarrier mapping has higher sum rate than interleaved subcarrier mapping in all cases. This is expected as interleaved subcarrier allocation creates roughly equivalent conditions for all users in each chunk, and the gain of chunk allocation will be less than that on localized FDMA where some users are more likely to experience stronger channels on some chunks due to the fading model with memory. The optimal maximum weighted matching algorithm, and the slightly less complex jointly greedy power user assignment achieve almost identical results, and the greedy user allocation performs nearly as well at much lower complexity, especially for the IFDMA scenario. The gain from optimum power allocation is much more pronounced for IFDMA with independent subcarrier fading, in other words with low number of taps, as in LFDMA, due to the correlation among the adjacent subcarriers, constant power allocation is already nearly optimal. However, when the number of taps increases of Rayleigh channel, the gain from optimum power allocation also makes sense. As a result, it can be concluded that power allocation is more vital for IFDMA in low number of taps, but is vital for both IFDMA and LFDMA in high number of taps. In addition, chunk allocation is more vital for LFDMA than IFDMA. Nevertheless, their joint use always produce the best results for any kind of number of taps.

Figures 5.6, 5.7, 5.8 and 5.9 illustrate the performance of the proposed algorithms for a system with 32 chunks as illustrated for a system with the 16 chunks. Same tone

spacing is used for this system, so the total bandwidth of the system is 10 MHz. As a result of the wider bandwidth, the total throughput is higher than the system with 5 MHz. There is no difference from the point of view of performance of proposed algorithms. The user diversity makes sense when the number of users exceeds 32.

In order to preserve fairness between the users, it is assumed that each user can only take one chunk in the system. User demands are out of scope of this thesis because the aim of the thesis is sum-rate capacity maximization. Therefore, the proposed optimal algorithm is derived from optimality conditions and the two suboptimal algorithms are derived to maximize sum-rate capacity with lower computational complexity. In addition, the system is assumed as overloaded which means the number of users is greater than the number of chunks, ($K > N$). Even though assigning N users to N chunks, there is $K - N$ users who have not been assigned to any chunk. The proposed algorithms are derived from instantaneous values. The proportional fairness may be considered with time varying systems.

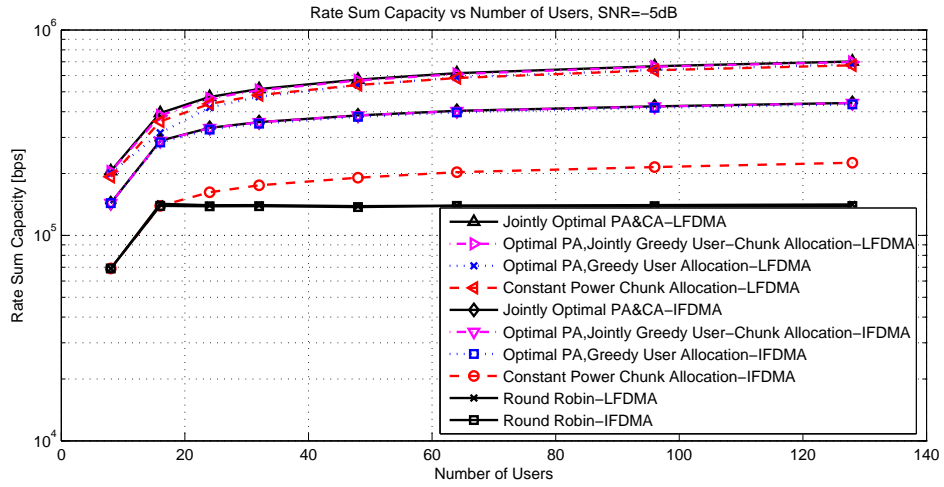


Figure 5.1: Sum rate of proposed algorithms (SNR=-5dB, $N=16$ chunks, $B=5$ MHz, $L=256$ subcarriers, 8-tap Rayleigh channel).

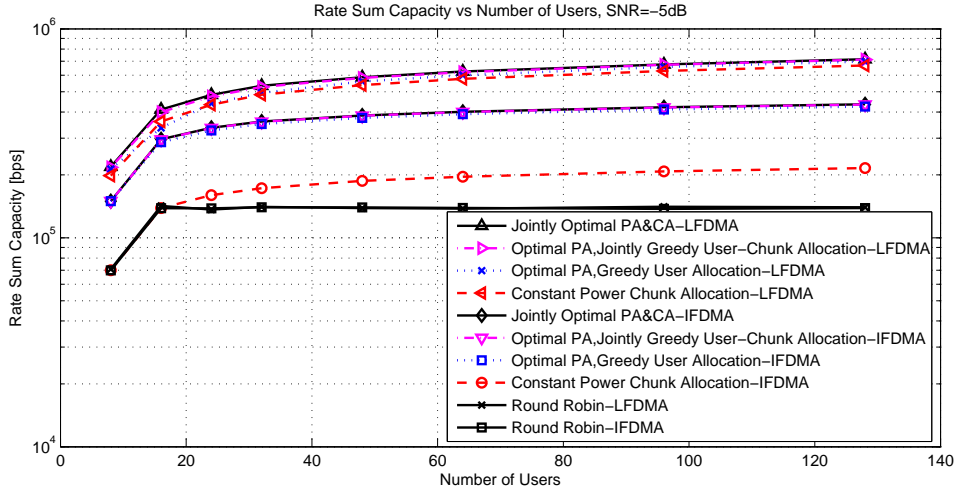


Figure 5.2: Sum rate of proposed algorithms (SNR=-5dB, $N=16$ chunks, $B=5$ MHz, $L=256$, subcarriers, 10-tap Rayleigh channel).

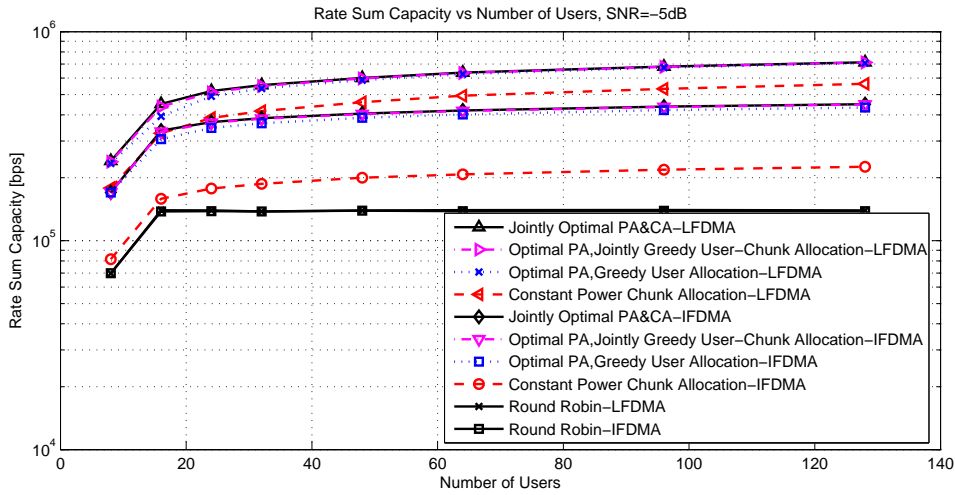


Figure 5.3: Sum rate of proposed algorithms (SNR=-5dB, $N=16$ chunks, $B=5$ MHz, $L=256$, subcarriers, 20-tap Rayleigh channel).

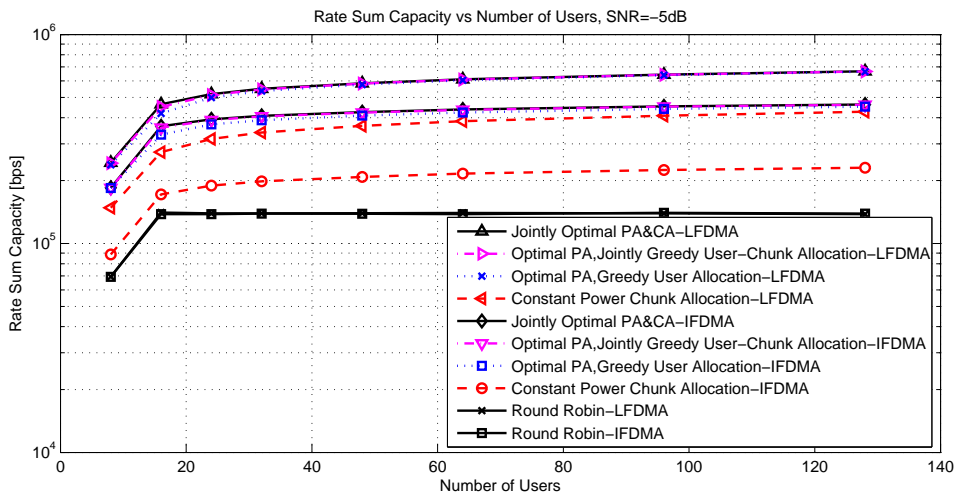


Figure 5.4: Sum rate of proposed algorithms (SNR=-5dB, $N=16$ chunks, $B=5$ MHz, $L=256$, subcarriers, 40-tap Rayleigh channel).

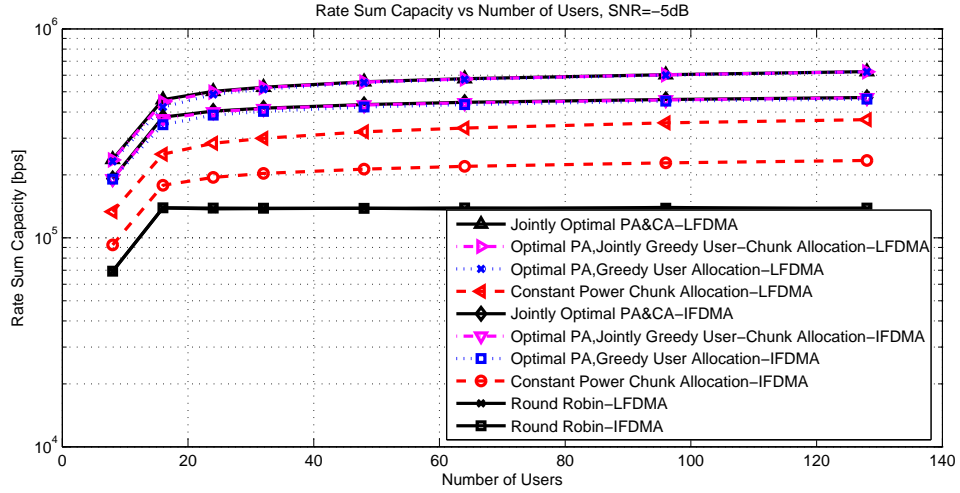


Figure 5.5: Sum rate of proposed algorithms (SNR=-5dB, $N=16$ chunks, $B=5$ MHz, $L=256$, subcarriers, 60-tap Rayleigh channel).

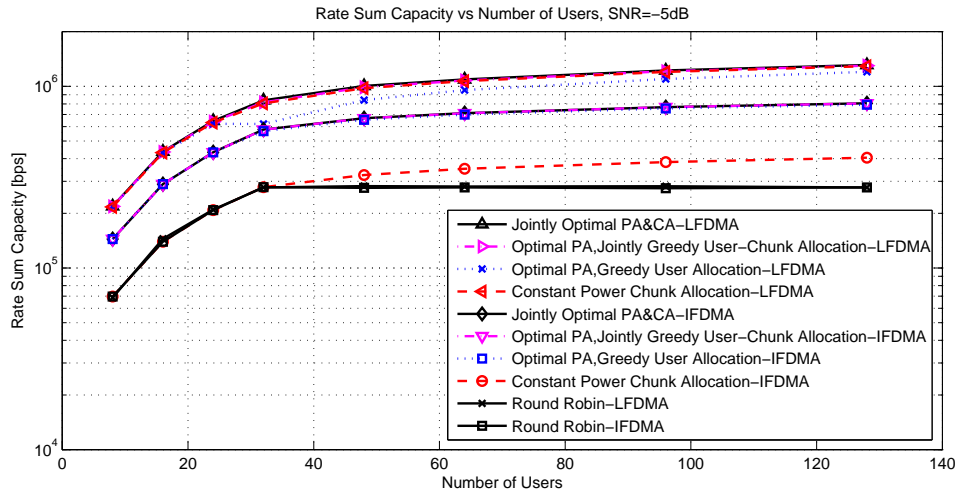


Figure 5.6: Sum rate of proposed algorithms (SNR=-5dB, $N=32$ chunks, $B=10$ MHz, $L=512$, subcarriers, 8-tap Rayleigh channel).

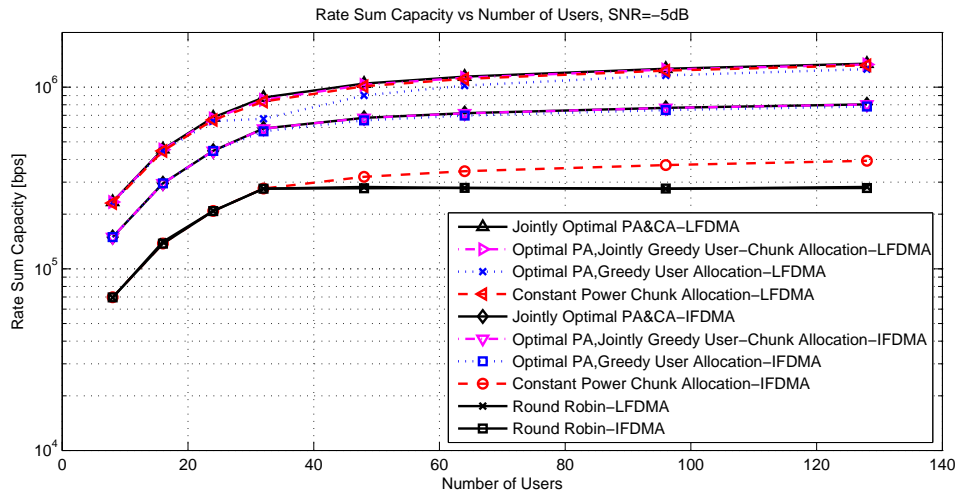


Figure 5.7: Sum rate of proposed algorithms (SNR=-5dB, $N=32$ chunks, $B=10$ MHz, $L=512$, subcarriers, 10-tap Rayleigh channel).

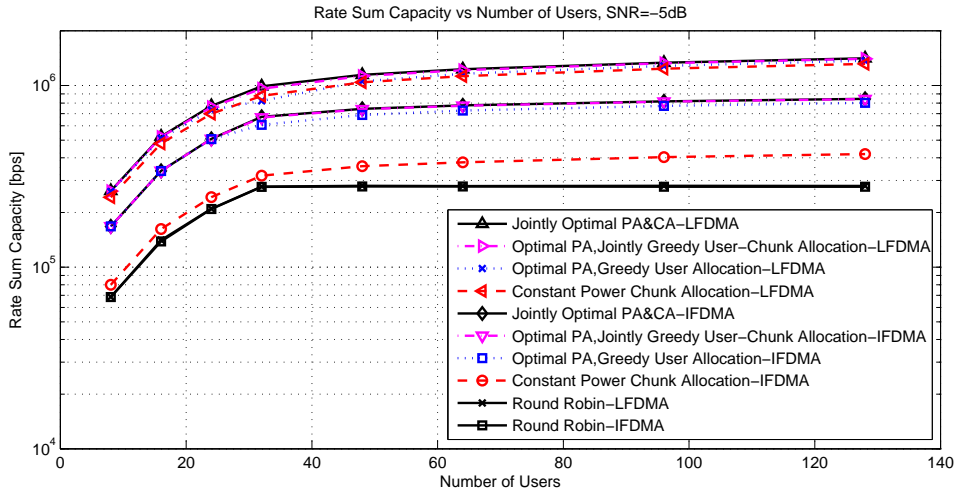


Figure 5.8: Sum rate of proposed algorithms (SNR=-5dB, $N=32$ chunks, $B=10$ MHz, $L=512$, subcarriers, 20-tap Rayleigh channel).

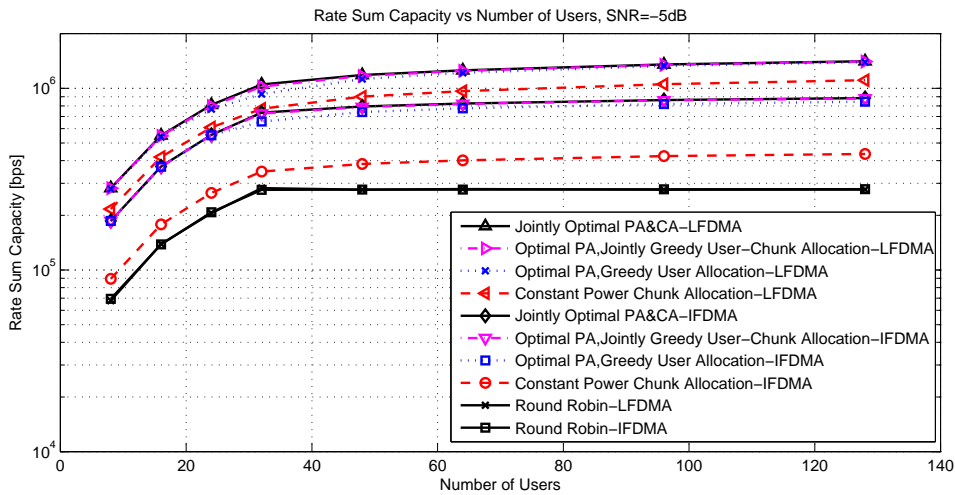


Figure 5.9: Sum rate of proposed algorithms (SNR=-5dB, $N=32$ chunks, $B=10$ MHz, $L=512$, subcarriers, 40-tap Rayleigh channel).

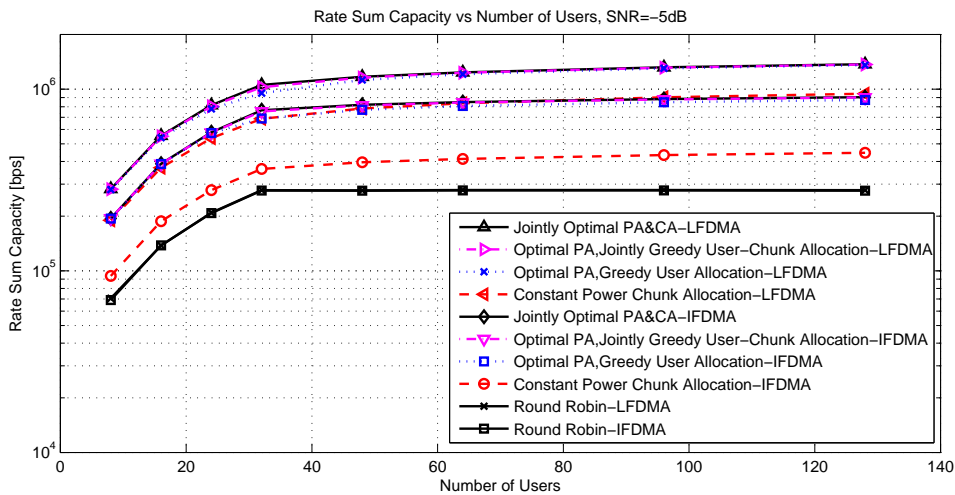


Figure 5.10: Sum rate of proposed algorithms (SNR=-5dB, $N=32$ chunks, $B=10$ MHz, $L=512$, subcarriers, 60-tap Rayleigh channel).

5.2 PAPR Analysis of Proposed Power Allocation Algorithm

The major advantage of SC-FDMA systems is low PAPR due to OFDMA systems. In order to maintain this kind of low PAPR of SC-FDMA systems, equal power allocation for each subcarrier of a particular chunk was proposed in [4]. However, allocating equal power to each subcarrier does not provide optimality conditions regarding power allocation. Therefore, sum-rate capacity can not be at maximum value for the user who is using a particular chunk. In this thesis, a power allocation algorithm is proposed which satisfies optimality conditions and increases sum-rate capacity to its maximum value for the user who is using the chunk. As a natural result of not allocating equal power to each subcarrier of a chunk, PAPR will increase. The motivation of this simulation is that how much the PAPR will increase the with proposed power allocation algorithm.

Monte Carlo simulation technique is used to demonstrate PAPR analysis of proposed power allocation algorithm comparing with allocating equal power to each subcarrier of a chunk. PAPR analysis is done for both localized and interleaved subcarrier mapping. In Figure 5.11, PAPR IFDMA power allocation curve represents power allocation algorithm with interleaved subcarrier mapping; PAPR LFDMA power allocation curve represents power allocation algorithm with localized subcarrier mapping; PAPR LFDMA no power allocation curve represents without power allocation (equal power to each subcarrier) with localized subcarrier mapping; PAPR IFDMA no power allocation curve represents without power allocation with interleaved subcarrier mapping.

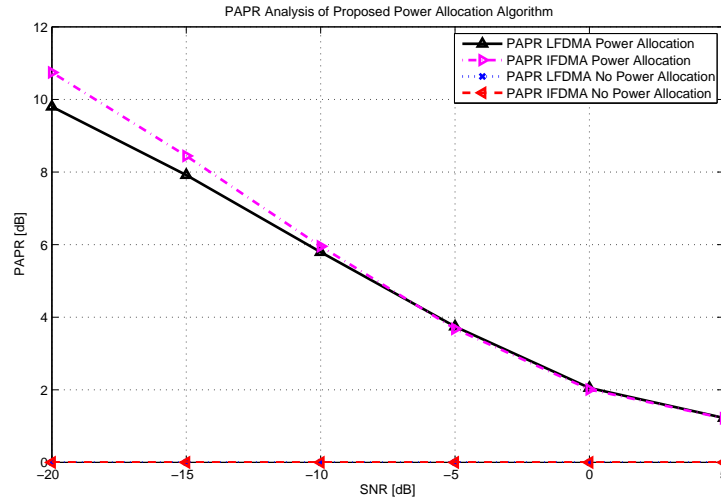


Figure 5.11: PAPR Analysis of proposed power allocation algorithm.

As it is shown in Figure 5.11, PAPR is very high when the SNR value is low. This kind of high PAPR will evaporate the advantage of SC-FDMA systems due to OFDMA systems. However, as the SNR value increases, PAPR decreases to ignorable values. No power allocation curves show 0 dB for every SNR value because equal power is assigned to each subcarrier which means peak power is equal to average power.

6. CONCLUSIONS AND FUTURE WORKS

SC-FDMA utilizes single carrier modulation, DFT-precoded orthogonal frequency multiplexing, and frequency domain equalization. It is a technique that has similar performance and essentially the same overall complexity as OFDMA. The most significant advantage over OFDMA is that the SC-FDMA signal has better peak power characteristics because of its inherent single carrier structure. SC-FDMA has drawn great attention as an attractive alternative to OFDMA, especially in the uplink communications of LTE, LTE-Advanced and WiMAX because transmit power efficiency is so critical for mobile terminals. Power amplifiers of transmitters do not need highly linear range in SC-FDMA systems so it is also cost effective due to power amplifiers of OFDMA systems.

In this thesis, the joint chunk and power allocation problem for an SC-FDMA system with frequency domain equalization was solved. The solution was performed in two steps, separating the power allocation and the chunk allocation steps; the latter of which was carried out using one optimal, and two suboptimal yet computationally more efficient approaches. It is demonstrated that, for both localized and interleaved subcarrier mapping that employing power control in conjunction with chunk allocation results in significant rate gains over known results, especially for IFDMA in a radio channel with lower memory, and both of IFDMA and LFDMA in a radio channel with higher memory. It is also further observed that, even with greedy algorithms for chunk allocation, near optimal solutions can be obtained, at much lower computational complexity.

It is also observed that when the number of user increases in a SC-FDMA system, the sum-rate also increases for both localized and interleaved subcarrier mapping because of user diversity providing that number of user is greater than number of chunks. In addition, localized subcarrier mapping provides multi-user diversity because of

frequency selectivity of radio channel and interleaved subcarrier mapping provides frequency diversity because the transmitted signal is spread over the entire bandwidth.

In the proposed algorithms for joint chunk and power allocation, it is assumed that each user can take only one chunk. For the future work, assigning more than one chunk to a user may be considered. It is a combinatorial problem, because even though assigning two chunks to a user, two questions arise: how we can decide which two chunks to select and how we can divide total power of user to the selected two chunks? In addition, alternative greedy algorithms may be obtained for chunk allocation at much lower computational complexity.

REFERENCES

- [1] **Wong, I. and Evans, B.**, 2008. Resource Allocation in Multiuser Multicarrier Wireless Systems, Springer.
- [2] **Myung, H.G., Lim, J. and Goodman, D.J.**, 2006. Single carrier FDMA for uplink wireless transmission, *Vehicular Technology Magazine, IEEE*, **1(3)**, 30–38.
- [3] **Myung, H., Lim, J. and Goodman, D.**, 2006. Peak-to-average power ratio of single carrier FDMA signals with pulse shaping, *Personal, Indoor and Mobile Radio Communications, 2006 IEEE 17th International Symposium on*, 1–5.
- [4] **Lim, J., Myung, H., Oh, K. and Goodman, D.**, 2006. Channel-dependent scheduling of uplink single carrier FDMA systems, *Vehicular Technology Conference, 2006. VTC-2006 Fall. 2006 IEEE 64th*.
- [5] **Jang, J. and Lee, K.B.**, 2003. Transmit power adaptation for multiuser OFDM systems, *Selected Areas in Communications, IEEE Journal on*, **21(2)**, 171–178.
- [6] **Ng, C.Y. and Sung, C.W.**, 2008. Low complexity subcarrier and power allocation for utility maximization in uplink OFDMA systems, *Wireless Communications, IEEE Transactions on*, **7(5)**, 1667–1675.
- [7] **Shen, Z., Andrews, J. and Evans, B.**, 2005. Adaptive resource allocation in multiuser OFDM systems with proportional rate constraints, *Wireless Communications, IEEE Transactions on*, **4(6)**, 2726–2737.
- [8] **Rhee, W. and Cioffi, J.**, 2000. Increase in capacity of multiuser OFDM system using dynamic subchannel allocation, *Vehicular Technology Conference Proceedings, 2000. VTC 2000-Spring Tokyo. 2000 IEEE 51st*, 1085–1089 vol.2.
- [9] **Gao, L. and Cui, S.**, 2008. Efficient subcarrier, power, and rate allocation with fairness consideration for OFDMA uplink, *Wireless Communications, IEEE Transactions on*, **7(5)**, 1507–1511.
- [10] **Wu, D., Cai, Y. and Pan, C.**, 2009. Joint subcarrier and power allocation in uplink OFDMA systems with incomplete channel state information, *Networks Security, Wireless Communications and Trusted Computing, 2009. NSWCTC '09. International Conference on*, 47–51.

- [11] **Thanabalasingham, T., Hanly, S., Andrew, L. and Papandriopoulos, J.**, 2006. Joint allocation of subcarriers and transmit powers in a multiuser OFDM cellular network, *Communications, 2006. ICC '06. IEEE International Conference on*, 269–274.
- [12] **Ng, C.Y. and Sung, C.W.**, 2008. Low complexity subcarrier and power allocation for utility maximization in uplink OFDMA systems, *Wireless Communications, IEEE Transactions on*, **7(5)**, 1667–1675.
- [13] **Wong, C.Y., Cheng, R., Lataief, K. and Murch, R.**, 1999. Multiuser OFDM with adaptive subcarrier, bit, and power allocation, *Selected Areas in Communications, IEEE Journal on*, **17(10)**, 1747–1758.
- [14] **Wong, I., Shen, Z., Evans, B. and Andrews, J.**, 2004. A low complexity algorithm for proportional resource allocation in OFDMA systems, *Signal Processing Systems, 2004. SIPS 2004. IEEE Workshop on*, 1–6.
- [15] **Mohanram, C. and Bhashyam, S.**, 2005. A sub-optimal joint subcarrier and power allocation algorithm for multiuser OFDM, *Communications Letters, IEEE*, **9(8)**, 685–687.
- [16] **Wong, C.Y., Cheng, R., Lataief, K. and Murch, R.**, 1999. Multiuser OFDM with adaptive subcarrier, bit, and power allocation, *Selected Areas in Communications, IEEE Journal on*, **17(10)**, 1747–1758.
- [17] **Kim, K., Han, Y. and Kim, S.L.**, 2005. Joint subcarrier and power allocation in uplink OFDMA systems, *Communications Letters, IEEE*, **9(6)**, 526–528.
- [18] **Myung, H., Oh, K., Lim, J. and Goodman, D.**, 2008. Channel-Dependent Scheduling of an Uplink SC-FDMA System with Imperfect Channel Information, *Wireless Communications and Networking Conference, 2008. WCNC 2008. IEEE*, 1860–1864.
- [19] **Lim, J., Myung, H., Oh, K. and Goodman, D.**, 2006. Proportional fair scheduling of plink single-carrier FDMA systems, *Personal, Indoor and Mobile Radio Communications, 2006 IEEE 17th International Symposium on*, 1–6.
- [20] **Wong, I., Oteri, O. and Mccoy, W.**, 2009. Optimal resource allocation in uplink SC-FDMA systems, *Wireless Communications, IEEE Transactions on*, **8(5)**, 2161–2165.
- [21] **Sokmen, F. and Girici, T.**, 2010. Uplink resource allocation algorithms for Single-Carrier FDMA systems, *Wireless Conference (EW), 2010 European*, 339–345.
- [22] **Pao, W.C. and Chen, Y.F.**, 2010. Chunk allocation schemes for SC-FDMA systems, *Vehicular Technology Conference (VTC 2010-Spring), 2010 IEEE 71st*, 1–5.
- [23] **Nwamadi, O., Zhu, X. and Nandi, A.**, 2008. Dynamic subcarrier allocation for single carrier FDMA systems, *European Signal Processing Conference, 2008*.

- [24] **Ruder, M., Ding, D., Dang, U.L. and Gerstacker, W.**, 2011. Combined user pairing and spectrum allocation for multiuser SC-FDMA transmission, *Communications (ICC), 2011 IEEE International Conference on*, 1–6.
- [25] **Huang, G., Nix, A. and Armour, S.**, 2007. Impact of radio resource allocation and pulse shaping on PAPR of SC-FDMA signals, *Personal, Indoor and Mobile Radio Communications, 2007. PIMRC 2007. IEEE 18th International Symposium on*, 1–5.
- [26] **Wang, M., Zhong, Z. and Liu, Q.**, 2011. Resource allocation for SC-FDMA in LTE uplink, *Service Operations, Logistics, and Informatics (SOLI), 2011 IEEE International Conference on*, 601–604.
- [27] **Goldsmith, A.**, 2005. *Wireless Communications*, Cambridge University Press, Cambridge, New York.
- [28] **Rappaport, T.S.**, 2002. *Wireless Communications: Principles and Practice*, Prentice Hall, 2nd edition.
- [29] **Cover, T.M. and Thomas, J.A.**, 2006. *Elements of Information Theory*, Hoboken, N.J.: Wiley-Interscience.
- [30] **Boyd, S.P. and Vandenberghe, L.**, 2004. *Convex Optimization*, Cambridge University Press, Cambridge, New York.
- [31] **Myung, H.G. and Goodman, D.J.**, 2008. *Single Carrier FDMA, A New Interface For Long Ter Evolution*, John Wiley and Sons, Ltd.
- [32] **Rumney, M.**, 2008. *3GPP LTE: Introducing Single Carrier FDMA*, Technical Report, Agilent.
- [33] **Shi, T., Zhou, S. and Yao, Y.**, 2004. Capacity of single carrier systems with frequency-domain equalization, *Emerging Technologies: Frontiers of Mobile and Wireless Communication, 2004. Proceedings of the IEEE 6th Circuits and Systems Symposium on*, 429–432 Vol.2.
- [34] **3GPP**, 2005. R1-050718:Simulation methodology for EUTRA UL:IFDMA and DFT-Spread-OFDMA, Technical Report.
- [35] **Lawler, E.L.**, 1976. *Combinatorial Optimization: Networks and Matroids*, Holt, Rinehart and Winston.

APPENDICES

APPENDIX A.1 : Projection of Obtained Concave Cost Function

8. APPENDIX A.1

The cost function **4.12** derived in Section 4.3 is a concave function and the constraints form a convex set. The cost function

$$\max_{p_{i,k}} \left[-\log_2 \left(1 - \frac{1}{|I_{n,k}|} \sum_{i \in I_{n,k}} \frac{p_{i,k}}{p_{i,k} + c_{i,k}} \right) \right], \quad (8.1)$$

is equivalent to

$$\min_{p_{i,k}} \left[\log_2 \left(1 - \frac{1}{|I_{n,k}|} \sum_{i \in I_{n,k}} \frac{p_{i,k}}{p_{i,k} + c_{i,k}} \right) \right]. \quad (8.2)$$

The logarithm can be omitted because a logarithm function is a concave function and minimizing a logarithm function is equivalent to minimizing interior of the logarithm. Thus, it can be said that

$$\min_{p_{i,k}} \left[1 - \frac{1}{|I_{n,k}|} \sum_{i \in I_{n,k}} \frac{p_{i,k}}{p_{i,k} + c_{i,k}} \right], \quad (8.3)$$

or

$$\max_{p_{i,k}} \left[\frac{1}{|I_{n,k}|} \sum_{i \in I_{n,k}} \frac{p_{i,k}}{p_{i,k} + c_{i,k}} \right]. \quad (8.4)$$

Let us define $f(p_{i,k})$ as follow

$$f(p_{i,k}) = \frac{p_{i,k}}{p_{i,k} + c_{i,k}}. \quad (8.5)$$

$1/|I_{n,k}|$ is a constant value, so it can be omitted when maximizing a function and the cost function can be rewritten for $\forall_{i,k}$ as

$$\max_{p_{i,k}, \forall_{i,k}} \sum_{i \in I_{n,k}} f(p_{i,k}). \quad (8.6)$$

For a particular subcarrier and a particular user, $p_{i,k}$, rest of the pair of users and subcarriers of $I_{n,k}$ act as constant values and derivative of them are zero. Let us focus on $f(p_{i,k})$, partial derivative

$$\frac{\partial f(p_{i,k})}{\partial p_{i,k}} = \frac{c_{i,k}}{(p_{i,k} + c_{i,k})^2}, \quad (8.7)$$

is always a non-negative function and second partial derivative

$$\frac{\partial f^2(p_{i,k})}{\partial^2 p_{i,k}} = \frac{-2c_{i,k}}{(p_{i,k} + c_{i,k})^3}, \quad (8.8)$$

is always negative. Thus $f(p_{i,k})$ is always monotone increasing concave function. This is valid for rest of the pair users and subcarriers of $I_{n,k}$ and sum of all of the $f(p_{i,k})$'s is also concave.

CURRICULUM VITAE



Name Surname:Teoman MERT

Place and Date of Birth:ARDAHAN, 25/08/1987

E-Mail:mertteo@gmail.com

B.Sc.:2005 - 2010, Dept. of Electrical and Electronics Engineering
Karadeniz Technical University

Professional Experience and Rewards:

- | | |
|-------------------|--|
| 01/2013 - present | NEC Telecommunication and Information Technology, LTD. Femtocell Solutions Engineer |
| 10/2010 - 12/2012 | Isik University, Faculty of Engineering, Department of Electrical and Electronics Engineering Research Assistant |
| 10/2011 - 08/2012 | TÜBİTAK Graduate Scholarship |
| June 5, 2010 | Karadeniz Technical University, Ranked 3 rd place in the university and 1 st place in the Faculty of Engineering |

List of Publications:

PUBLICATIONS/PRESENTATIONS ON THE THESIS

- **Mert, T.**, Kaya, O. and Çırpan, H., 2013. Jointly Optimal Chunk and Power Allocation in Uplink SC-FDMA, *IEEE International Conf. of Communications 2013*, June 9-13, 2013 Budapest, Hungary.